Imperial College London

Department of Physics

An introduction to Quantum Chromodynamics and the structure of nucleon

Author
Emilie LI

Supervisor
Dr. Samuel WALLON

Submitted in partial fulfilment of the requirements for the degree of Master of Science of Imperial College London.

October 23, 2020

Contents

List of Figures

Abstract

In this dissertation, the basic features of Quantum Chromodynamics as the non-abelian gauge theory for strong interaction are presented before exploring how one can probe the structure of the nucleons using leptons-nuclons scattering. The important concept of partons as point-like constituents of hadrons, will be introduced along with the notion of form factors and parton distribution functions. Predictions form pertrbative QCD will be compared to experiment data of the last fifty years.

Acknowledgements

First and foremost, I would like to greatly thank my supervisor, Samuel Wallon for his guidance during the project and for pointing out the directions to go forward. I would also like to thank Lech Szymanowski for his help to make me better understand the parton model.

I would also like to express my gratitude to all the lecturers in the theoretical physics group for their amazing lectures throughout the year and some PhD students for their explanations of the things I was confused about.

Finally, I would like to thank my friends for their continuous support and my parents, without whom this year would not have been possible.

Chapter 1

Introduction

1.1 Introduction

At the end of the 1960s, experiments at Stanford Linear Accelerator Center (SLAC) have shown that at the high energy limit, the cross-section of deep inelastic scattering (DIS) on a lepton on a nucleons has the same form as the differential cross-section for $e^-\mu^- \to e^-\mu^-$, meaning that the proton appears as a point-like particle. Moreover, the structure functions of nucleons, that encode their inner structure seems to satisfy a scaling law. In the same moment, Feynman [16] and Bjorken [8] develop the parton model, model where the nucleons are composed of point-like particles, the partons. This gives an intuitive explanation of SLAC experimental results. At the time, the specific nature of these particles was unknown. Experimental data suggested that the charged partons have spin $1/2$ and the measure of the momentum carried by them leads to a postulate on the possible existence of neutral partons, which would carry the unobserved fraction of momentum.
A few years later, the theory of Quantum Chromodynmaics (QCD) was developed by Gell-Mann, Fritzsch and Leutwyler. They were inspired by the discovery that non-Abelian gauge theories can have the property of asymptotic freedom, which leads in QCD to confinement. Within this gauge theory of strong interaction, quarks have a new quantum number called colour. The charged partons were then going to be identified as quark and anti quark while the neutral ones as gluons.
Many questions on this theory and also on the structure of hadrons, still remain and a lot has yet to be discovered. I will focus on the determination of the structure of nucleon in this thesis. Form factors (FFs) and parton distribution functions (PDFs) are two ways to gain information on their structure. The latter is the distribution of longitudinal momentum of partons while the former are distribution of charge.
After introducing the basis of QCD and its quantisation, the aim of this thesis is to give an understanding of form factors and parton distribution functions through the examination of lepton-nucleon scattering.

Before discussing further on these, I will first list some properties and results that would be of use in further chapters.

1.2 The S-Matrix

First of all, when analysing any physical processes, the optical theorem and Cutkosky rules facilitate the computation of cross-section and of the scattering amplitude of the associated Feynman diagrams.

1.2.1 Optical theorem

One of the property of the S-matrix is to be unitary. This comes from the conservation of probability: the probability that an in-state scatters into an out state and then summing over all possible out-states should give one. This leads to the optical theorem.

$$\begin{aligned} S^\dagger S = SS^\dagger = \mathbb{1} \\ (\mathbb{1} - iT^\dagger)(1 + iT) = \mathbb{1} \\ \left(T^\dagger\right)_{fn} T_{ni} = -i\left(T - T^\dagger\right)_{fi} \\ \sum_n \mathcal{M}^*_{nf}\mathcal{M}_{ni}(2\pi)^4\delta^{(4)}(P_n - P_i) = -i(\mathcal{M}_{fi} - \mathcal{M}^*_{if}). \end{aligned}$$

If $i = f$ has an elastic scattering, then:

$$\sum_n |\mathcal{M}_{ni}|^2(2\pi)^4\delta^{(4)}(P_n - P_i) = 2\,\mathrm{Im}(\mathcal{M}_{ii}). \tag{1.1}$$

The total cross-section for the process $i \to X$ is related to the forward elastic scattering amplitude through the expression:

$$\sigma_{tot} = \frac{1}{2\sqrt{\lambda(s, m_1^2, m_2^2)}}\,\mathrm{Im}(\mathcal{M}_{ii}(s, t = 0)), \tag{1.2}$$

with $\lambda(s, m_1^2, m_2^2) = \left[s - (m_1 + m_2)^2\right]\left[s - (m_1 - m_2)^2\right]$, m_1 and m_2 are the masses of the two initial particles.

In the case of massless particles or if the masses are neglected, then: $\lambda(s, 0, 0) = s^2$.

1.2.2 Cutkosky rules

These rules allow us to easily calculate the imaginary part of the scattering amplitude for a G diagram, which is related to the discontinuity of the Feynman amplitude in the s-channel through the relation:

$$\mathrm{Im}(T_{if}) = \Delta T_{if} = \frac{1}{2i}\,\mathrm{Disc}\,T_{if} \equiv \lim_{\epsilon \to 0}\left[T_{if}(s + i\epsilon) - T_{if}(s - i\epsilon)\right]. \tag{1.3}$$

The definition of the discontinuity comes from the fact that the S-matrix is an analytic function [18].

Schematically, the rules can be represented by figure 1.1.

The steps to calculate the discontinuity or imaginary part of a diagram are the following:

1. Cut the internal lines of the diagram in all the possible ways that the internal particles can be put in shell.

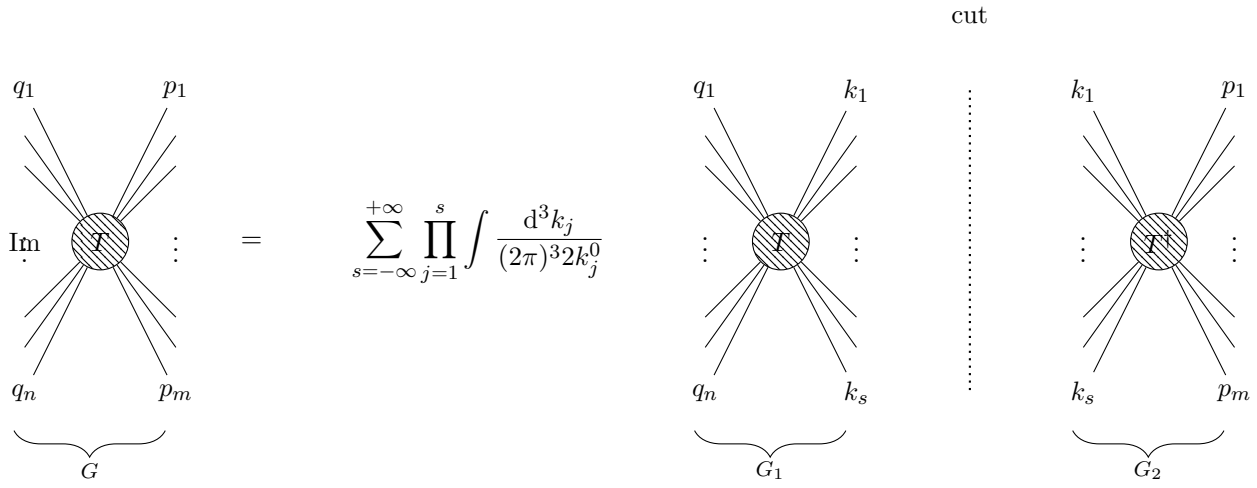

Figure 1.1: Cutkosky rules

2. For each cut, the propagators $1/\left(p^2 - m^2 + i\epsilon\right)$ is replaced by $-2\pi i\delta(p^2 - m^2)$. This replacement comes from the residue theorem that states that $\mathrm{Disc}\left(1/\left(k^2 \pm i\epsilon\right)\right) = \mp 2\pi i\delta(k^2)$. The numerators of the cut propagators are not changed. We then do a product of all the cuts.

3. For the left part G_1, the usual Feynman rules apply for the internal lines and vertices. For the right part G_2, the rules are conjugated. Therefore, the Feynman prescription for G_2 is with $-i\epsilon$.

4. We integrate over all possible loops even the one which are cut.

5. A final sum over all the possible ways of cutting is then realised.

In the case of a scalar field, for a given cut n, the following steps would give

$$\begin{aligned}\Delta T_{if(G)} &= \frac{1}{2} T_{in(G_1)} T^{\dagger}_{nf(G_2)} \prod_{k_j \in \mathrm{cut}\, n} (2\pi)\theta\left(k_j^0\right)\delta\left(k_j^2 - m_j^2\right) \\ &= \frac{1}{2}(-i)^{V_1 - V_2} \int \prod_{i}^{L} \frac{d^4 q_l}{(2\pi)^4} \prod_{I_1=1}^{I_1} \frac{i}{k_{l_1}^2 - m_{l_1}^2 + i\varepsilon} \prod_{I_2=1}^{I_2} \frac{-i}{k_{l_2}^2 - m_{l_2}^2 - i\varepsilon} \prod_{I_1+I_2+1}^{I} (2\pi)\theta\left(k_j^0\right)\delta\left(k_j^2 - m_j^2\right),\end{aligned} \tag{1.4}$$

with I, I_1, I_2 the number of internal lines for G, G_1 and G_2, V_1 and V_2 the number of vertices in the left and right part and L the total number of loops. Here, the Heaviside function imposes $k_j^0 > 0$, ensuring that cuts are in the physical region of the scattering amplitude.

1.3 Results from QED processes

In this section, we briefly analyse two quantum electrodynamics (QED) processes, which results will be uselful when studying QCD processes at quark level.

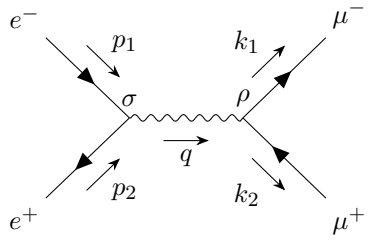

Figure 1.2: Annihilation $e^+e^- \to \mu^-\mu^+$

1.4 $e^+e^- \to \mu^+\mu^-$ results

The amplitude of the Feynman diagram 1.4 is

$$i\mathcal{M} = (\bar{v}(p_2)(-ie\gamma^\sigma)u(p_1))\,\frac{-ig_{\rho\sigma}}{q^2}\,(\bar{u}(k_1)(-ie\gamma^\rho)v(k_2)) \tag{1.5}$$

For the unpolarized process, we sum over the spin of the outgoing particles and average over the incoming *incoming?*. This leads to the definition of the leptonic tensors.

$$\frac{1}{4}\sum_{\text{spins}}|\mathcal{M}|^2 = \frac{e^4}{4q^4}\,\mathrm{Tr}\{(\not{p}_1 + m_e)\gamma^\sigma(\not{p}_2 - m_e)\gamma^\rho\}\,\mathrm{Tr}\{(\not{k}_2 - m_\mu)\gamma_\sigma(\not{k}_1 + m_\mu)\gamma_\rho\} \tag{1.6}$$

$$= \frac{e^4}{q^2}\ell^{\sigma\rho}_{(e)}\ell_{(\mu)\sigma\rho} \tag{1.7}$$

Using the Gamma matrix trace properties, the leptonic tensors read:

$$\ell^{\sigma\rho}_{(e)} \equiv \frac{1}{2}\,\mathrm{Tr}\{(\not{p}_1 + m_e)\gamma^\sigma(\not{p}_2 - m_e)\gamma^\rho\} = 2\left[p_1^\sigma p_2^\rho + p_1^\rho p_2^\sigma - g^{\rho\sigma}(p_1.p_2 + m_e^2)\right] \tag{1.8}$$

$$\ell_{(\mu)\sigma\rho} \equiv \frac{1}{2}\,\mathrm{Tr}\{(\mu)\gamma_\sigma(\not{k}_1 + m_\mu)\gamma_\rho\} = 2\left[k_{1\sigma}k_{2\rho} + k_{1\rho}k_{2\sigma} - g_{\rho\sigma}(k_1.k_2 + m_\mu^2)\right] \tag{1.9}$$

The equation (1.7) becomes then

$$\frac{1}{4}\sum_{spin}|\mathcal{M}|^2 = \frac{8e^4}{s^2}\left[(p_1.k_1)(p_2.k_2) + (p_1.k_2)(p_2.k_1) + m_\mu^2(p_1.p_2) + m_e^2(k_1.k_2) + 2m_e^2m_\mu^2\right] \tag{1.10}$$

We neglect now the mass of the electron and the positron compared to all other quantities and note by E their energy and θ the scattering angle.

In the center of mass frame, (1.10) becomes:

$$\frac{1}{4}\sum_{\text{spins}}|\mathcal{M}|^2 = e^4\left[1 + \frac{m_\mu^2}{E^2} + \left(1 - \frac{m_\mu^2}{E^2}\right)\cos^2\theta\right] \tag{1.11}$$

As a reminder, the differential cross section for the unpolarized process $1 + 2 \to 3 + 4$ in the center of mass frame reads:

$$\frac{\mathrm{d}\sigma}{\mathrm{d}\Omega} = \frac{p_f}{p_i}\frac{1}{64\pi^2 s}\frac{1}{4}\sum_{\text{spins}}|\mathcal{M}|^2 \tag{1.12}$$

With p_i and p_f the momentum of the incoming and outgoing particles respectively.

Using (1.12), the differential cross-section reads :

$$\frac{\mathrm{d}\sigma}{\mathrm{d}\Omega} = \frac{\alpha^2}{4s}\sqrt{1-\frac{m_\mu^2}{E^2}}\left[1+\frac{m_\mu^2}{E^2}+\left(1-\frac{m_\mu^2}{E^2}\right)\cos^2(\theta)\right] \tag{1.13}$$

with θ is the scattering angle.

Integrating (1.12) over $\mathrm{d}\Omega = \mathrm{d}\phi\mathrm{d}\cos(\theta)$ gives finally the total cross section:

$$\sigma_{tot}(e^-e^+ \to \mu^-\mu^+) = \frac{4\pi\alpha^2}{3s}\sqrt{1-\frac{m_\mu^2}{E^2}}\left[1+\frac{1}{2}\frac{m_\mu^2}{E^2}\right] \tag{1.14}$$

In the high energy limit, i.e. $E >> m_\mu$, this becomes

$$\sigma_0 = \frac{4\pi\alpha^2}{3s} \tag{1.15}$$

1.4.1 $e^-\mu^- \to e^+\mu^-$ scattering

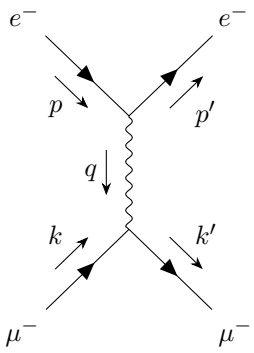

Figure 1.3: Diffusion $e^-\mu^- \to e^-\mu^-$

The amplitude of $e^-\mu^-$scattering, represented by 1.4.1 can be obtained by crossing symmetry to the $e^+e^- \to \mu^+\mu^-$ process, with the change of variables:

$$p_1 = p, \quad p_2 = -p', \quad k_1 = k \quad \text{and} \quad k_2 = -k', \tag{1.16}$$

one obtains, from (1.6),

$$\begin{aligned}\frac{1}{4}\sum_{\text{spins}}|\mathcal{M}|^2 &= \frac{e^4}{q^4}\frac{1}{2}\,\mathrm{Tr}\left[\left(-\not{p}' - m_e\right)\gamma^\rho\left(\not{p}+m_e\right)\gamma^\sigma\right]\frac{1}{2}\,\mathrm{Tr}\left[\left(\not{k}'+m_\mu\right)\gamma_\rho\left(-\not{k}-m_\mu\right)\gamma_\sigma\right] \\ &= \frac{8e^4}{q^4}\left[\left(p\cdot k'\right)\left(p'\cdot k\right)+\left(p\cdot k\right)\left(k'\cdot k'\right)-m_\mu^2\left(p\cdot p'\right)-m_e^2\left(k\cdot k'\right)+2m_e^2m_\mu^2\right].\end{aligned} \tag{1.17}$$

The expression (1.17) can be simplified when going to the laboratory frame:

$$p = (E,\vec{p}\,), \quad p' = \left(E',\vec{p}'\right), \quad k = (m_\mu, 0), \tag{1.18}$$

giving then:

$$\frac{1}{4}\sum_{\text{spins}}|\mathcal{M}|^2 = \frac{16e^4}{q^4}m_\mu^2EE'\left[\cos^2\frac{\theta}{2}+\frac{Q^2}{2m_\mu^2}\sin^2\frac{\theta}{2}\right]. \tag{1.19}$$

In the laboratory frame, the differential cross-section has the general expression ,

$$\frac{d\sigma}{d\Omega} = \frac{E_3^2}{m_2^2E_1^2}\frac{1}{64\pi^2}|\mathcal{M}|^2 \tag{1.20}$$

From (1.20), the differential cross-section in the laboratory frame reads:

$$\frac{d\sigma}{d\Omega}\left(e^-\mu^- \to e^-\mu^-\right) = \frac{\alpha^2}{4E^2\sin^4\frac{\theta}{2}}\frac{E'}{E}\left[\cos^2\frac{\theta}{2} + \frac{Q^2}{2m_\mu^2}\sin^2\frac{\theta}{2}\right]. \tag{1.21}$$

1.5 Outline

In Chapter 2, I will first go through some basics on QCD before talking about the important property of asymptotic freedom. As the distance between quarks increases, so is the strong coupling constant. In reverse, at high energies or short distances, quarks behave as free particle. This leads, in QCD, to confinement, meaning that only colorless states are observable. Chapter 3 is split into three sections. In the first one, I will give some generalities on lepton-nucleon scattering. I will then study the case of elastic scattering, that allows measures of form factors. The last section is an examination of deep inelastic scattering within the parton model, giving access to parton distribution functions.

Chapter 2

The basics of Quantum Chronodynamics

The conventions are those of Peskin-Schroeder [33].

2.1 QCD Lagrangian

Quantum chromodynamics is a local gauge theory, based on the color group $SU(3)_c$ and involve quark fields ψ and eight massless spin-1 gluons vector bosons $A^a_\mu, a = 1, ..., 8$.

Omitting spinor indices on the quark fields and noting by and i, j the color indices, the classical QCD Lagrangian takes the form:

$$L = -\frac{1}{2}\,\mathrm{Tr}(F_{\mu\nu a}F^{\mu\nu a}) + \sum_{colors} \bar{\psi}_i(i\not{D} - m)_{ij}\psi_j$$

where

$$(D_\mu)_{ij} = \delta_{ij}\partial_\mu - igA^a_\mu t^a_{ij} \tag{2.1}$$

$$F_{\mu\nu} \equiv \frac{i}{g}[D_\mu, D_\nu] = \partial_\mu A_\nu - \partial_\nu A_\mu + \frac{i}{g}[A_\mu, A_\nu] \tag{2.2}$$

t^a are called the generators of $SU(3)_c$ such that $U = e^{it^a\alpha^a} \in SU(3)$. They are hermitian traceless matrices in order to satisfy $U^\dagger U = \mathbb{1}$ and $\det(U) = 1$. They also respect the Lie algebra $[t^a, t^b] = if^{abc}t^c$, where f^{abc} are the structure constants. In the fundamental representation, those generators also respect the orthonormality condition : $Tr(t^a t^b) = \frac{1}{2}\delta^{ab}$.

From the Lie algebra, we have for the component of the field strength

$$F^a_{\mu\nu} = \partial_\mu A^a_\nu - \partial_\nu A^a_\mu + g f^{abc} A^b_\mu A^c_\nu$$

Finally, the gauge fields are in the Lie algebra and transform as :

$$A_\mu \to UA_\mu U^{-1} - \frac{i}{g}(\partial_\mu U)U^{-1} = UA_\mu U^{-1} + \frac{i}{g}(\partial_\mu U^{-1})U$$

The infinitesimal form of the transformation

$$\delta A^a_\mu = \frac{1}{g}(D_\mu)^{ab}\alpha^b$$

with the covariant derivative in the adjoint representation of SU(3).

2.2 Quantisation of QCD

2.2.1 Fadeev-Papoov approch to quantisation

The quantisation of the QCD Lagrangian will use the path integral approach instead of the old-fashioned method of canonical quantisation (see appendix B). The difficulty in quantising the QCD Lagrangian does not come from the fermionic part but from the Yang-Mills part of the Lagrangian. This is because, compared to the case of QED, the gluons are self-interacting, a consequence of the fact that the Lie group is not abelian. Let's then focus on the quantisation of $L_{YM} = -\frac{1}{2}Tr(F_{\mu\nu a}F^{\mu\nu a})$.

Naively, the sourceless generating function would be defined as :

$$Z[0] = \int DA_\mu \ \exp\left(i\int \mathrm{d}^4x \, \frac{1}{4}(F^a_{\mu\nu})^2\right) \tag{2.3}$$

where $\int DA_\mu = \prod_x \prod_a \int \mathrm{d}A^a_\mu(x)$

However, this definition is not compatible with the gauge invariance requirement. If we have $A^a_\mu = B^a_\mu + \frac{1}{g}D_\mu\theta^a$ such that $B^a_0 = 0$ and by gauge invariance of $F^a_{\mu\nu}$ ($F_{\mu\nu}$ independent of θ), this leads to:

$$\begin{aligned} Z[0] &= \int DA_\mu \int D\theta \ \exp\left(i\int \mathrm{d}^4x \, \frac{1}{4}(F^a_{\mu\nu})^2\right) \\ &= \int DA_\mu \ \exp\left(i\int \mathrm{d}^4x \, \frac{1}{4}(F^a_{\mu\nu})^2\right) \int D\theta \end{aligned}$$

$\int D\theta$ corresponds to the volume of the gauge orbit and is an infinite constant that cannot be cancelled in any way. Therefore, (2.3) cannot work as the definition of the generating function.

The correct definition of the sourceless generating function should be :

$$Z_{new}[0] = \frac{Z[0]}{\int D\theta} \tag{2.4}$$

The path integral expression of this sourceless generating function is found using the Fadeev-Papov de Witt approach.

The first step of this approach is to fix the gauge : $F^a(A^\theta_{a\mu}) = 0 = G^\mu A^{a\theta}_\mu = G^\mu(A^a_\mu + D_\mu\theta)$. The solution to $F^a(A^\theta_{a\mu}) = 0$ is noted θ^*.

Different choices of gauge exist depending on the choice of G_μ:

$$G_\mu = \begin{cases} \partial_\mu & \text{Lorenz gauge} \\ (0, \vec{\nabla}) & \text{Coulomb gauge} \\ n_\mu & \text{axial gauge. The usual choice of unit vector is } n_\mu = (0,0,0,1) \end{cases}$$

The next step is to insert $\int D\theta \ \delta(\theta - \theta^*) = 1 = \int D\theta \ \left|\det\left(\frac{\delta F^a(A^\theta_\mu(x))}{\delta\theta^b(y)}\right)\right| \ \delta(F^a(A^\theta_\mu))$ in the old expression of the generating function.

Thus, (2.3) is rewritten as :

$$Z[0] = \int DA_\mu \int D\theta \ \left|\det\left(\frac{\delta F^a(A^\theta_\mu(x))}{\delta\theta^b(y)}\right)\right| \ \delta(F^a(A^\theta_\mu)) \exp\left(i\int \mathrm{d}^4x \, \frac{1}{4}(F^a_{\mu\nu})^2\right) \tag{2.5}$$

Using the fact that the only elements that depend on θ are the A^θ_μ in the delta function and Jacobian, one can make the change of notation $A^\theta_\mu \to A_\mu$. As a result, the integrand is completely independent of θ. Moreover, the functional integral of A_μ is not modified by this change. Hence, the functional integral $\int D\theta$ can be factorized.

Thus, (2.4) has the expression :

$$Z[0] = \int DA_\mu \ \left|\det\left(\frac{\delta F^a(A_\mu)(x)}{\delta\theta^b(y)}\right)\right| \ \delta(F^a(A_\mu)) \exp\left(i\int \mathrm{d}^4x \, \frac{1}{4}(F^a_{\mu\nu})^2\right) \tag{2.6}$$

The last step of the process is to express the delta function and Jacobian in terms of new fields.

For the delta function, analog to the Fourier transformation form, we can write:

$$\delta(F^a(A_\mu)) = \int DB^a \ \exp\left(i\,\mathrm{d}^4x \, B^a F^a(A_\mu)\right) = \int DB^a \ \exp\left(i\int \mathrm{d}^4x \, B^a G^\mu A^a_\mu\right) \tag{2.7}$$

The Jacobian is expressed with a Grassmann integration :

$$\left|\det\left(\frac{\delta F^a(A_\mu)(x)}{\delta\theta^b(y)}\right)\right| = \int Dc \int D\bar{c} \ \exp\left(\int \mathrm{d}^4x \, \mathrm{d}^4y \ \bar{c}^a(y)\frac{\delta F^a(A_\mu(x))}{\delta\theta^b(y)}c^b(y)\right) \tag{2.8}$$

At the end, inserting expressions (2.7) and (2.8) in (2.6) and the quark fields and using $\frac{\delta F^a(A^\theta_\mu(x))}{\delta\theta^b(y)} = \delta(x-y)G_\mu D^{\mu ab}$:

$$Z[0] = \int DA_\mu \int DB \int Dc \int D\bar{c} \int D\psi \int D\bar{\psi} \ \exp\left\{i\int \mathrm{d}^4x \ (L_{BRST} + L_F)\right\} \tag{2.9}$$

with $L_{BRST} = \frac{1}{4}(F^a_{\mu\nu})^2 + B^a G^\mu A^a_\mu + \bar{c}^a G_\mu (D^\mu c)^a$ and $L_F = \bar{\psi}(i\not{D} - m)\psi$

2.2.2 BRST symmetry

The introduction of the ghost fields makes the BRST Lagrangian not gauge invariant anymore. However, a new symmetry appears which is the BRST symmetry :

$$\begin{cases} \delta\bar{c}^a = & -\epsilon B^a \\ \delta A^a_\mu = & \epsilon D_\mu c^a \\ \delta c^a = & -\epsilon\frac{g}{2} f^{abc} c^b c^c \\ \delta B = & 0 \\ \delta\psi = & \epsilon i g c^a t^a \psi \end{cases}$$

with ϵ a Grassmann variable. It is conventional to work with δ_B defined as $\delta = \epsilon\delta_B$.
This symmetry has an important property which is that it is nilpotent ie $\delta_B^2 = 0$ With this property, we can add any term of the form $\delta_B G$ in the BRST action without changing the physics. The common choice is to choose $G = -\frac{1}{2}\xi\bar{c}B$ which gives $\delta_B G = -\frac{1}{2}\xi B^{a2}$.

After addition to this new term, we can then perform the B path integral equation:

$$\int DB \quad \exp\left(i\int \mathrm{d}^4x\,\frac{1}{2}\xi B^{a2} + B^a G_\mu A^{\mu a}\right) = \mathcal{N}\exp\left(-i\int \mathrm{d}^4x\,\frac{(G_\mu A^{\mu a})^2}{2\xi}\right)$$

with $\mathcal{N}$ renormalisation constant. This leads to a gauge fixing term in the new form of BRST Lagrangian that will be used from now on: $L_{BRST} = L_{YM} + L_{GF} + L_{FP}$, with

$$\begin{cases} L_{YM} = & -\frac{1}{4}F^a_{\mu\nu}F^{\mu\nu a} \\ L_{GF} = & -\frac{1}{2\xi}(G_\mu A^{\mu a})^2 \\ L_F P = & \bar{c}G_\mu(D^\mu c)^a \end{cases} .$$

We have two possible expressions for the gauge fixing term. The first one is the covariant form $L_{GF} = -\frac{1}{2\xi}(\partial_\mu A^{\mu a})^2$ and the second one is the axial gauge fixing term $L_{GF} = -\frac{1}{2\xi}(n_\mu A^{\mu a})^2$. In the latter case, if n_μ is chosen such that $n_\mu A^\mu = 0$ then there is no interaction between the ghost fields and the gauge fields i.e. the ghost fields do not couple to any physical degree of freedom. Hence, the ghost fields could be ignored.

2.2.3 Ghost fields and unitarity of the S-matrix

However, in the case of covariant gauge, the presence of ghost fields is crucial to preserve the unitarity of the S-matrix. This statement can be made explicit using the optical theorem for fermion-anti fermion annihilation as shown in more details in [33].

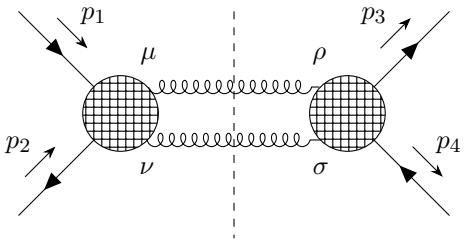

Figure 2.1: Quark anti-quark annihilation diagram and Cutkosky rules

Let's define new polarisation vectors for the gauge fields : $\epsilon_i^\mu(k)$ for $i \in 1, 2$ are the two transverse polarisation vectors i.e. $\epsilon.k = 0$. For the other two unphysical polarization, we define the forward polarisation vector $\epsilon_\mu^+(k) = \frac{1}{\sqrt{2}|\underline{k}|}k_\mu$ and the backward polarisation vector $\epsilon_\mu^-(k) = \frac{1}{\sqrt{2}|\underline{k}|}k_\mu = \frac{1}{\sqrt{2}|\underline{k}|}\tilde{(k^0, -\underline{k})}$. The metric could then be expressed in terms of these polarisation vectors : $g_{\mu\nu} = \epsilon_\mu^-\epsilon_\nu^{+*} + \epsilon_\mu^+\epsilon_\nu^{-*} - \epsilon_\mu^i\epsilon_{i\nu}^*$.

From the Cutkosky rules, the diagram 2.1 gives a contribution of

$$\frac{1}{2}4\pi^2\delta(k_1^2)\delta(k_2^2)(i\mathcal{M}^{\mu\nu}g_{\rho\mu}g_{\nu\sigma}\mathcal{M}'^{\rho\sigma}), \tag{2.10}$$

where $\mathcal{M}^{\mu\nu}$ is the scattering amplitude for $q\bar{q} \to gg$ and $\mathcal{M}'^{\rho\sigma}$ is the scattering amplitude for the reverse process. k_1 and k_2 are momentum on the gluons internal lines.

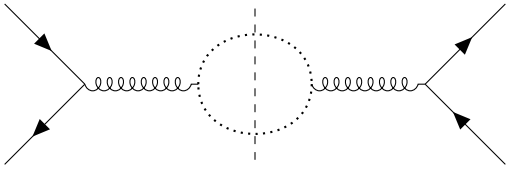

Figure 2.2: Ghost contribution in quark -anti quark annihilation

Almost all combination of polarization vectors $\epsilon_\rho(k_1)\epsilon^*_\mu(k_1)\epsilon^*_\nu(k_2)\epsilon_\sigma(k_2)$, when contracted with the scattering amplitudes $\mathcal{M}^{\mu\nu}\mathcal{M}'^{\rho\sigma}$ gives 0, by computation. For example,

$$i\mathcal{M}^{\mu\nu}\epsilon^*_\nu(k_2)\epsilon^{+*}_\mu(k_1) = -\frac{1}{\sqrt{2}|\underline{k_1}|}\frac{g^2}{s}\bar{v}(p_2)t^c \not{k}_2 u(p_1) f^{abc} k_2^\nu \epsilon^*_\nu(k_2)$$

and so with $\epsilon^*_\nu(k_2)$ a transverse polarization vector, the contribution is therefore null. The only two combinations that give a non-vanishing value when contracting with the scattering amplitude are $\epsilon^+_\rho \epsilon^{-*}_\mu \epsilon^{+*}_\nu \epsilon^-_\sigma$ and the one composed of only transverse polarization. The second combination does not cause any issue for the optical theorem as they are physical polarization. On the contrary, the first one is unphysical. When using the optical theorem, this would mean that one can have final gluons as final states with unphysical polarizations, which should be impossible.

Using the Dirac equation for the spinor constants, the unphysical contribution is equal to :

$$\frac{g^4}{s^2}(\bar{\nu}(p_2)\gamma_\mu t^c u(p_1) f^{abc} k_1^\mu)(\bar{u}(p_3)\gamma_\rho t^d \nu(p_4) f^{abd}(-k_2^\rho)) \tag{2.11}$$

The ghost loop contribution corresponding to the diagram 2.2 compensate exactly (2.11).

Thus, through this simple example of fermion-anti-fermion annihilation, one can see that the presence of ghost fields, which only appear in internal loop in Feynman diagrams is indispensable to preserve unitarity of the S-matrix.

2.2.4 Feynman rules

The different propagators necessary in the study of QCD are first listed below. We note a, b, i, j the SU(3) indices, with i,j for the fundamental representation and a,b for the adjoint representation.

The fermionic propagator is:

$j \xrightarrow{p} i$ $\qquad \frac{i}{(\not{p} - m)}\delta_{ij} = \frac{i(\not{p} + m)}{p^2 - m^2 + i\epsilon}\delta_{ij}$ with the $i\epsilon$ Feynman prescription (2.12)

In the case of the covariant gauge, we have the gauge-field and the ghost-field propagators to take into account.

For the gauge fields, we have :

$a \xrightarrow{p} b$ $\qquad D^{ab}_{\mu\nu}(p) = \delta_{ab}\frac{-i}{p^2 + i\epsilon}(g_{\mu\nu} - (1-\xi)\frac{p_\mu p_\nu}{p^2})$ (2.13)

The Landau gauge corresponds to $\xi = 0$ and the Feynman gauge corresponds to $\xi = 1$. It is only in the former gauge that $p_\mu D^{\mu\nu}(p) = 0$.

For the ghost fields, we have :

$b \xrightarrow{p} a$ $\qquad \frac{-i}{p^2 + i\epsilon}\delta_{ab}$ (2.14)

For the axial gauge where we can neglect the ghost fields, we have:

$$D^{ab}_{\mu\nu} = \frac{-i}{p^2 + i\varepsilon}\left[g_{\mu\nu} - \frac{n_\mu p_\nu + p_\mu n_\nu}{n\cdot p} + \frac{\xi p^2 + n^2}{(n\cdot p)^2} p_\mu p_\nu\right]\delta^{ab} \tag{2.15}$$

It is easy to see that

$$p_\mu D^{\mu\nu}(p) = 0 \quad \text{for} \quad p^2 = 0 \tag{2.16}$$

One special example of non-covariant gauge (also called "physical gauge") is the light-cone gauge where $n^2 = 0$ and $\xi = 0$. In this particular gauge, the free gluon propagator is :

$$D^{ab}_{\mu\nu} = \frac{-i}{p^2 + i\varepsilon}\left[g_{\mu\nu} - \frac{n^\mu p^\nu + p^\mu n^\nu}{n\cdot p}\right]\delta^{ab} \tag{2.17}$$

This propagator respects both (2.16) and $n_\mu D^{\mu\nu}(p) = 0$, meaning that we have only the transverse polarization as physical polarization.

Using the fact that the decomposition of the metric in the basis $\{p_\mu, n_\mu, \epsilon_i\}$ is as follows:

$$g_{\mu\nu} = g^\perp_{\mu\nu} + \frac{1}{(n.p)}(p_\mu n_\nu + p_\nu n_\mu) - \frac{p^2}{(n.p)^2} n_\mu n_\nu$$

where $g^\perp_{\mu\nu} = -\sum_{i=1}^{2} \epsilon^*_{i\mu}\epsilon_{i\nu}$, (2.17) can be rewritten as:

$$D_{\mu\nu} = \frac{-i}{p^2 + i\varepsilon}\left[g^\perp_{\mu\nu} - p^2\frac{n_\mu n_\nu}{(p\cdot n)^2}\right] \tag{2.18}$$

The different vertices that appear in Feynman diagrams are :

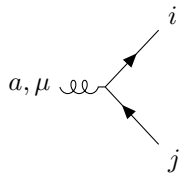

$$ig\gamma^\mu t^a_{ij}$$

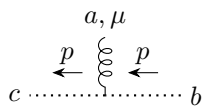

$$-gf^{abc}p^\mu$$

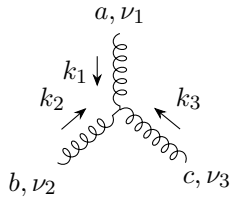

$$V^{\nu_1\nu_2\nu_3}_{abc}(k_1,k_2,k_3) = gf^{abc}\left[g^{\nu_1\nu_2}(k_1-k_2)^{\nu_3} + g^{\nu_2\nu_3}(k_2-k_3)^{\nu_1} + g^{\nu_1\nu_3}(k_3-k_1)^{\nu_2}\right]$$

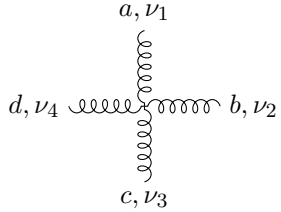

$$\begin{aligned}&-ig^2\left[f^{abe}f^{cde}\left(g^{\nu_1\nu_3}g^{\nu_2\nu_4} - g^{\nu_1\nu_4}g^{\nu_2\nu_3}\right) + f^{ace}f^{bde}\left(g^{\nu_1\nu_2}g^{\nu_3\nu_4} - g^{\nu_1\nu_4}g^{\nu_2\nu_3}\right)\right.\\ &\left.+ f^{ade}f^{bce}\left(g^{\nu_1\nu_2}g^{\nu_3\nu_4} - g^{\nu_1\nu_3}g^{\nu_2\nu_4}\right)\right]\end{aligned}$$

These vertices are found by calculating the corresponding vacuum expectation value of the operators at tree levels, e.g. the three-point function $\langle\Omega|\widehat{T}A^a_{\nu_1}(x)A^b_{\nu_2}(y)A^c_{\nu_3}(z)|\Omega\rangle$ for the three-gluon vertex.

2.3 Asymptotic freedom

The discovery and experimental proof with SLAC of the approximate Bjorken scaling, that will be studied in the next chapter, has stressed the importance for theoretical physicist to find an explanation for this phenomenon, resulting in the discovery of asymptotic freedom for non-abelian gauge theories, by Gross and Wilczek [19] and Politzer [34]. They also proved that an asymptotically-free renormalizable theory is only possible with non-Abelian gauge fields. This discovery was key in the development of QCD.

Using renormalisation group theory, they computed the β-function in Yang-Mills theory, including fermions and found its expression, at first order.

The gauge field contribution to the β-function reads:

$$\beta_V = -\frac{g^3}{(4\pi)^2}\frac{11}{3}C_A \tag{2.19}$$

with C_A the quadratic Casimir operator in the adjoint representation. The minus sign means that as the energy increases, the strong coupling constant decreases. Therefore, (2.19) is the proof of asymptotic freedom.

An explicit calculation to find β_V using the background field method is presented in the appendix C.

The fermion contribution to the *beta*-function is

$$\beta_F = \frac{g^3}{(4\pi)^2}\frac{4}{3}T_R n_R \tag{2.20}$$

where $Tr(T^a T^b) = T_R \delta_{ab}$ and n_R is the number of flavour of fermions in the representation R.

In the special case of SU(3), the β-function is therefore

$$\beta = -\frac{g^3}{(4\pi)^2}(11 - \frac{2}{3}n_F) = -\frac{g^3}{(4\pi)^2}b_0 \tag{2.21}$$

where $n_F = n_R$. (2.21) implies that the theory is asymptotically free if the number of flavour of fermions is sufficiently small $n_F \leq 16$.

(2.21) leads to the expression below of the strong coupling constant $\alpha_S = \frac{g^2}{4\pi}$:

$$\alpha_s\left(\mu^2\right) = \frac{4\pi}{b_0 \log \frac{\mu^2}{\Lambda^2_{QCD}}} \tag{2.22}$$

where μ^2 the energy scale.

Currently, the β-functions are known to five-loop order [3].

An explanation of asymptotic freedom can be given when one talks about screening and anti-screening caused by gluons and pairs of quark-anti quark. In the QCD vacuum, the gauge bosons are present as gluons can self-interact, making the vacuum into a paramagnetic medium ie $\mu > 1$. Moreover, in quantum field theory, the dielectric constant and magnetic permeability are related by $\mu\epsilon = 1$. Hence, $\epsilon < 1$, resulting in anti-screening by gluons. On the opposite, the quark-anti quark pair, just like for electron-positron pair in Quantum Electrodynamics, are screening the color charge. As long as the anti-screening from gluons overshadows the screening from quark-anti quark, the color charge therefore increases with the distance from it and QCD is an asymptotically -free theory [29].

2.4 $e^+e^- \to$ Hadrons process

At high energy, the total cross-section process $e^+e^- \to Hadron$ is calculated using the total cross-section of the process $e^+e^- \to q\bar{q}$.

Moreover, the cross-section of $e^+e^- \to q\bar{q}$ is related to the one for the process $e + e^- \to \mu^+\mu^-$ through the R-ratio defined as:

$$R = \frac{\sigma_{tot}\left(e^+e^- \to q\bar{q}\right)}{\sigma_{tot}\left(e^+e^- \to \mu^+\mu^-\right)} \tag{2.23}$$

At Born level i.e. tree-level in quantum field theory,

$$R^{(0)} = N_c \sum_f e_f^2 = 3\sum_f e_f^2, \tag{2.24}$$

where the sum is over the quark flavour and e_f is the electric charge of the quark of flavour f.

Hence, considering the three-quarks up, down and strange only, the R-ratio is

$$R^{(0)}_{u,d,s} = 3\left[\left(\frac{2}{3}\right)^2 + \left(\frac{-1}{3}\right)^2 + \left(\frac{-1}{3}\right)^2\right] = 2.$$

If one includes the charm quarks, this then becomes

$$R^{(0)}_{u,d,s,c} = 3\left[\left(\frac{2}{3}\right)^2 + \left(\frac{-1}{3}\right)^2 + \left(\frac{-1}{3}\right)^2 + \left(\frac{2}{3}\right)^2\right] = \frac{10}{3}.$$

2.4.1 Leading radiative corrections to the total cross section

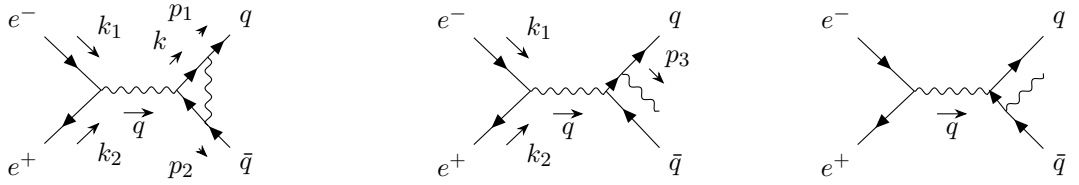

Figure 2.3: Corrections of order α_S to the proccess $e^-e^+ \to$ hadrons

The first-order correction comes from the exchange of soft gluons and the emission of collinear gluons represented in Figure 2.3.

For the following scattering amplitude, we use the covariant gauge and Feynman gauge. The first diagram corresponds to the scattering amplitude

$$i\mathcal{M} = (-ie)^2 e_f\left(\bar{v}(k_1)\gamma^\rho u(k_1)\right)\frac{-ig_{\rho\sigma}}{q^2}\int\frac{\mathrm{d}^d k}{(2\pi)^d}\bar{u}(p_1)(ig\gamma^\mu t^a)\frac{i\not{k}}{k^2}\gamma^\sigma\frac{i(-\not{q}+\not{k})}{(q-k)^2}(ig\gamma^\nu t^b)v(p_2)\frac{-ig_{\mu\nu}}{(k-p_1)^2}\delta^{ab} \tag{2.25}$$

The sum of the contributions of the last two diagrams gives the scattering amplitude

$$i\mathcal{M} = e_f(-ie)^2(ig)\left(\bar{v}(k_2)\gamma_\rho u(k_1)\right)\epsilon^*_\nu(p_3)\bar{u}(p_1)\left[t^a\gamma^\nu\frac{i}{\not{p}_1+\not{p}_3}\gamma^\rho - \gamma^\rho\frac{i}{\not{p}_2+\not{p}_3}\gamma^\nu t^a\right] \tag{2.26}$$

One finds that they give a correction to the total cross-section of the form

$$\sigma(e^-e^+ \to q\bar{q}, q\bar{q}g) = \sigma_0 R^{(0)}\left(1 + \frac{\alpha_S}{\pi} + O(\alpha_S^2)\right) \tag{2.27}$$

where σ_0 is given by (1.15). The expression above can be improved if one replaces α_S, defined at a specific renormalisation point, by $\alpha_S(\sqrt(s))$ defined by (2.22).

In the total cross-section, the infrared divergences of the form $\alpha_S \ln\left(\frac{\mu^2}{s}\right)$ and $\alpha_S \ln^2\left(\frac{\mu^2}{s}\right)$, with μ the "mass of the gluon" (i.e. an explicit regulator), that are present for the exchange and emission of gluons individually, disappear when summing all contributions. This is a consequence of the Kinoshita-Nauenberg-Lee (KNL) theorem which says that the Standard model is infrared finite and that the infrared divergences from final states are cancelled when summing over all the degenerancy. The cancellation of infrared divergence can also be understood when considering the time scales. Indeed, the tree-level process $e^-e^+ \to q\bar{q}$ takes $\tau = \frac{1}{\sqrt{s}}$ with $s = q^2$. The life time of the virtual final states represented in figure 2.3 have a life time of $T = \frac{1}{p_{g\perp}}$, with $p_{g\perp} << \sqrt{s}$ the transverse momentum of the collinear gluons with respect to the $q\bar{q}$ system. As $\tau << T$, these final virtual states and infra-red divergences do not affect the perturbative part of the cross-section of $e^+e^- \to hadrons$, meaning the subprocess $e^-e^+ \to q\bar{q}$, but can only affect the types of hadrons after hadronisation.

2.4.2 Jets production

The process $e^-e^+ \to q\bar{q}$ leads to 2-jets events by hadronisation. The quarks and anti quarks produced with limited transverse momentum and opposite momenta in the center-of-mass frame, are bound by the strong force, producing then quark-anti quark pairs. They will also absorb and emit gluons. This goes on until everything becomes hadrons. The 2-jets formed are in the direction of the initial quark and anti-quark.

The e^-e^+ collider SPEAR at SLAC provided the first experimental evidences of 2-jet events. Comparing the experimental results with Monte-Carlo simulations, the distribution of hadrons was found to be in good agreement with the jet model rather than an isotropic distribution [23].

One should expect the angular distribution for $e^-e^+ \to q\bar{q}$ to have the same form (1.13) as for the production of μ pair:

$$\frac{d\sigma\left(e^+e^- \to q\bar{q}\right)}{d\cos\theta} \propto 1 + \cos^2\theta \tag{2.28}$$

For the process $e^-e^+ \to q\bar{q}g$, the number of jets depends on the transverse momentum $p_{g\perp}$ of the gluons. If the transverse momentum is small i.e. the gluon emitted is collinear, then it will have no effect and we expect two jets back-to-back after hadronisation. However, if $p_{g\perp} \geqslant 1\text{GeV}$, we expect 3-jet events and its cross-section in QCD perturbation theory reads :

$$\frac{d\sigma}{dx_1 dx_2}\left(e^+e^- \to q\bar{q}g\right) = \sigma_0 \cdot \left(3\sum_f Q_f^2\right) \cdot \frac{2\alpha_s(p_{g\perp})}{3\pi} \frac{x_1^2 + x_2^2}{(1-x_1)(1-x_2)} \tag{2.29}$$

with x_i for $i = 1, 2, 3$ the ratio of the center-of-mass energy of the quark, anti quark and gluon to the electron-positron beam energy, $x_i = (2k_i \cdot q)/q^2$ with k_i the momentum of the final i particle and $q = k_1 + k_2 + k_3$. They satisfy $0 < x_i < 1$ and $\sum_i x_i = 2$.

Another way to examine jet-events is to work directly with them instead of talking about quark, anti quark and gluons as Sterman and Weinberg have done [41].

Chapter 3

The structure of the nucleons with lepton-nucleon scattering

The discussion that follows on the study of the structure of nucleons by the electron-nucleons mainly proton process is based on the notes by M. Samuel Wallon [37].

3.1 Generalities

As said in the introduction, one important problem yet to be solved in the study of hadrons is the characterization of their structure, in particular the structure of nucleons. The diffusion of a lepton (here, an electron but it could also be a muon) on a nucleon (here, a proton) is the historic process that helped the development of one key ingredients for their characterization, the form factors. It also led to the parton model and to the parton distribution functions. This electron-proton scattering process will be the focus of this chapter. After some general information on this diffusion, the next section will be about form factor in the elastic regime of this process.The last section will be dedicated to the inelastic case.

3.1.1 Kinematics

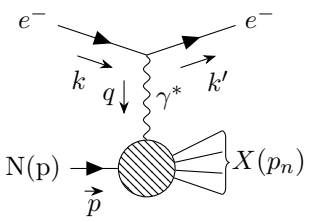

Figure 3.1: Electron-proton scattering

The lepton mass is neglected for this scattering. We note M the mass of the proton.

The invariant variables used to study the scattering as depicted in 3.1 are

$$q^2 = (k - k')^2 = -Q^2 \tag{3.1}$$

$$\nu = \frac{p.q}{M} \tag{3.2}$$

$$x_{Bj} = \frac{Q^2}{2p.q}, \quad 0 \leqslant x_{Bj} \leqslant 1 \tag{3.3}$$

$$W^2 = p_n^2 = (p + q)^2 = -Q^2 + 2M\nu + M^2 \geqslant M^2 \tag{3.4}$$

$$y = \frac{q.p}{k.p}, 0 \leqslant y \leqslant 1 \tag{3.5}$$

$$S = (k + p)^2 \tag{3.6}$$

where W^2 is the center-of-mass energy of the γ^* (or Z^0)-nucleons and x_{Bj} is the Bjorken variable.

Various relationships exist between those variables

$$Q^2 = 2M\nu x_{Bj} \tag{3.7}$$

$$W^2 = M^2 + Q^2(\frac{1}{x_{Bj}} - 1) \tag{3.8}$$

$$S = \frac{Q^2}{x_{Bj}y} + M^2 \tag{3.9}$$

Those variables are better understood in the proton rest frame, which kinematics is:

$$p_\mu = (M, 0, 0, 0), \quad k_\mu = (E, \vec{k}), \quad k'_\mu = \left(E', \vec{k'}\right) \tag{3.10}$$

We then have $\nu = E - E'$, that is to say that ν is the loss of energy for the lepton. Moreover, in this frame, we can see easily that the exchanged photon or boson is either space-like or light-like as

$$q^2 = \left(k - k'\right)^2 \simeq -2k \cdot k' = -4EE' \sin^2 \frac{\theta}{2} = 2MEx_{Bj}y \leq 0 \tag{3.11}$$

We also observe that $y = \frac{\nu}{E} = \frac{E-E'}{E}$ which corresponds to the fraction of energy lost by the incoming electron.

3.1.2 The different regimes of study

Different regimes of interest characterised by the three variables x_{Bj}, W^2 and Q^2 allow us to extract different properties and information on the structure of the proton. The first regime is the Mott regime where $Q^2 \sim 0$. In this case, $E \simeq E'$ and the proton is considered as point-like.

The second regime of study is the quasi-elastic one characterized by $Q^2(1 - x_{Bj}) << M^2$ or equivalently by $W^2 \simeq M^2$ from the relation (3.8). If the condition is respected, then $X(p_n) = N(p')$ meaning that the final product is the incoming proton in an excited state. The quasi-elastic scattering can be divided into two sub-regions. If $Q^2 \sim M^2$, we study form factors that give global information on the proton and more specifically give access to charge distribution radius. If $Q^2 >> M^2$ and x_{Bj} near 1, we are in the deep elastic region and one can predict the asymptotic behaviour of the form factors.

In general, if $Q^2 >> M^2$, the scattering is said to be deep and we can access information on the internal structure of the nucleon and its constituents. When $Q^2 >> \Lambda^2_{\text{QCD}}$ too, perturbative QCD can then be

used to predict scattering results and properties. The Deep Inelastic region corresponds to $W^2 >> M^2$, $Q^2 >> M^2$ and x_{BJ} not near 1. Finally, if $W^2 >> Q^2 >> M^2$, it is the perturbative Regge limit or small-x_{Bj} regime.

Before examining the scattering in these various regimes, I will first derive the general expression of the differential cross-section.

3.1.3 Cross-section and hadronic tensor

Cross-section

We suppose Q^2 small enough w.r.t $M_{Z^0}^2$ in order to consider that the particle exchanged in the t-channel is a photon.

The scattering amplitude for the process is

$$\mathcal{M}_n = e^2 \bar{u}\left(k', \lambda'\right) \gamma^\mu u(k, \lambda) \frac{1}{q^2} \left\langle n \left| J_\mu^{em}(0) \right| p, \sigma \right\rangle \tag{3.12}$$

with J_μ^{em} the hadronic part of the electromagnetic current and λ, λ', σ the spin of the incoming and outgoing electron and the proton.

The unpolarized differential cross-section has the expression

$$d\sigma_n = \frac{1}{2M2E} \frac{d^3k'}{(2\pi)^3 2k'_0} \prod_{i=1}^{n} \frac{d^3k_i}{(2\pi)^3 2k_{i0}} \frac{1}{4} \sum_{\sigma\lambda\lambda'} |\mathcal{M}_n|^2 (2\pi)^4 \delta^4\left(p + k - k' - p_n\right), \tag{3.13}$$

where $p_n = \sum_{i=1} k_i$i and $\mathcal{M}$ is given by (3.12).

If measures are taken only on the scattered lepton then the process is inclusive. To have the corresponding differential cross-section, one needs to integrate over the final hadronic system. Then, we have

$$d\sigma = \frac{e^4}{q^4} \frac{1}{2E} \frac{d^3k'}{(2\pi)^3 2k'_0} 2\pi W^{\mu\nu} \ell_{\mu\nu}^{(e)} \tag{3.14}$$

$\ell_{\mu\nu}^{(e)}$ is the leptonic tensor given by (1.8) and $W_{\mu\nu}$ is the hadronic tensor

$$W_{\mu\nu} = \frac{1}{4M} \sum_\sigma \sum_n \int \prod_{i=1}^{n} \frac{d^3k_i}{(2\pi)^3 2k_{i0}} \left\langle p, \sigma \left| J_\mu^{em} \right| n \right\rangle \left\langle n \left| J_\nu^{em} \right| p, \sigma \right\rangle (2\pi)^3 \delta^4 \left(p_n - p - q\right) \tag{3.15}$$

Finally, this leads to the simplified expression of the differential cross-section.

$$\frac{d^2\sigma}{d^2\Omega dE'} = \frac{\alpha^2}{q^4} \frac{E'}{E} \ell_{\mu\nu}^{(e)} W^{\mu\nu}. \tag{3.16}$$

The structure of the hadronic tensor

The most general form for this symmetric tensor, in terms of $g^{\mu\nu}$, q and p, is

$$W^{\mu\nu} = -W_1 g^{\mu\nu} + \frac{W_2}{M^2} p^\mu p^\nu + \frac{q^\mu q^\nu}{M^2} W_3 + \frac{p^\mu q^\nu + q^\mu p^\nu}{M^2} W_4. \tag{3.17}$$

There is no term with $\epsilon_{\mu\nu\rho\sigma}$ by parity conservation.

As for $\ell^{(e)}_{\mu\nu}$, $W^{\mu\nu}$ should respect current conservation $q_\mu W^{\mu\nu}$. This leads to

$$W_3 = \frac{M^2}{q^2} W_1 + \left(\frac{p\cdot q}{q^2}\right)^2 W_2 \quad \text{and} \quad W_4 = -\frac{p\cdot q}{q^2} W_2 \tag{3.18}$$

Therefore, the hadronic tensor has the expression

$$W^{\mu\nu}(p,q) = -W_1\left(g^{\mu\nu} - \frac{q^\mu q^\nu}{q^2}\right) + \frac{W_2}{M^2}\left(p^\mu - \frac{p\cdot q}{q^2}q^\mu\right)\left(p^\nu - \frac{p\cdot q}{q^2}q^\nu\right) \tag{3.19}$$

W_1 and W_2 are the nucleon structure function.

The hadronic and leptonic tensors can be decomposed into terms in a basis of projectors orthogonal to q_μ and p_μ, facilitating the computation of their contraction.

We define the transverse projector

$$T^{\mu\nu} = g^{\mu\nu} - \frac{q^\mu q^\nu}{q^2} \tag{3.20}$$

and longitudinal projector

$$L^{\mu\nu} = \frac{q^\mu q^\nu}{q^2} \tag{3.21}$$

such that $T^{\mu\nu}q_\nu = 0$, $L^{\mu\nu}q_\nu = q^\mu$ and $g^{\mu\nu} = T^{\mu\nu} + L^{\mu\nu}$.

The transverse projector can be further decomposed into

$$T^{\mu\nu} = P_L^{\mu\nu} + g_\perp^{\mu\nu}, \tag{3.22}$$

$g_\perp^{\mu\nu}$ projects to the subspace orthogonal to p_μ and q_μ while $P_L^{\mu\nu}$ projects into the remaining subspace.

One can express the two previous projectors in terms of photon polarisation vectors:

$$P_L^{\mu\nu} = \epsilon_L^\mu \epsilon_L^\nu \tag{3.23}$$

$$g_\perp^{\mu\nu} = -\sum_{i=1,2} \epsilon^{(i)\mu}\epsilon^{(i)\nu *} \tag{3.24}$$

where ϵ_L^μ is the longitudinal polarization vector and has the expression ,

$$\epsilon_L^\mu = \frac{1}{\sqrt{M^2 - \frac{(p\cdot q)}{q^2}q^\mu}} \tag{3.25}$$

and $\epsilon^{(i)\mu}, i = 1,2$ are the transverse polarization vectors. They have the following properties:

$$\epsilon^{(i)*}\cdot\epsilon^j = -\delta^{ij}, \quad \epsilon^i\cdot\epsilon_L = 0, \quad \epsilon_L^2 = +1$$

In terms of projector, (3.19) becomes

$$W^{\mu\nu}(p,q) = -W_1 T^{\mu\nu} + \left(1 - \frac{(p\cdot q)^2}{M^2 q^2}\right) W_2 P_L^{\mu\nu} \tag{3.26}$$

or

$$W^{\mu\nu}(p,q) = -W_1 g_\perp^{\mu\nu} + \left[-W_1 + \left(1 - \frac{(p\cdot q)^2}{M^2 q^2}\right) W_2\right] P_L^{\mu\nu} \tag{3.27}$$

To calculate the differential cross-section, one needs to calculate the contraction of the leptonic tensor

with the projectors.

$$\begin{aligned}\ell^{(e)}_{\mu\nu}P_L^{\mu\nu} &= \ell^{(e)}_{\mu\nu}\frac{p^\mu p^\nu}{M^2-\frac{(p\cdot q)^2}{q^2}} + (\text{terms} \propto q^\mu \ell^{(e)}_{\mu\nu} = 0)\\ &= \frac{2}{M^2\left(1-\frac{(p\cdot q)}{q^2}\right)}\left(3(k'\cdot p)(k\cdot p)+\frac{q^2}{2}M^2\right)\\ &\overset{lab}{=} \frac{4EE'\cos^2\frac{\theta}{2}}{1-\frac{(p\cdot q)^2}{M^2q^2}}\end{aligned}$$

and

$$\begin{aligned}\frac{1}{2}\ell_{\mu\nu}T^{\mu\nu} &= \frac{1}{2}\ell_{\mu\nu}\left(g^{\mu\nu}-L^{\mu\nu}\right)\\ &= q^2\\ &\overset{lab}{=} -4EE'\sin^2\frac{\theta}{2}\end{aligned}$$

Hence, in the laboratory frame,

$$\ell^{(e)}_{\mu\nu}W^{\mu\nu} = 4EE'\left[2W_1\sin^2\frac{\theta}{2}+W_2\cos^2\frac{\theta}{2}\right] \tag{3.28}$$

This results in

$$\frac{d^2\sigma}{d\Omega dE'} = \frac{\alpha^2}{4E^2\sin^4\frac{\theta}{2}}\left[2W_1\sin^2\frac{\theta}{2}+W_2\cos^2\frac{\theta}{2}\right] \tag{3.29}$$

In the last section, we will see that the measure of structure functions are a way to access to the measure of parton distribution functions. They also have some interesting properties in the context of naive parton model. But before getting into the model in details, I will first examine the quasi-elastic regime and the properties of form factors.

3.2 Elastic scattering

3.2.1 Hadronic current and form factors

When an electron scatters to an arbitrary charge distribution instead of a point like particle, the cross section of the process can be found by weighing the cross-section of a point-like particle with the amplitude of a form factor

$$\frac{d\sigma}{d\Omega} = \left(\frac{d\sigma}{d\Omega}\right)_{\text{point}}|F(q)|^2 \tag{3.30}$$

The form factor accounts for the inner structure, i.e. the fact that the particle is not point-like.

Moreover, if the photon exchanged is static i.e. $q^0 = 0$, it can be shown that

$$F(\mathbf{q}) = \int d^3x\rho(\mathbf{x})e^{i\mathbf{q}\cdot\mathbf{x}}. \tag{3.31}$$

Expanding around $|\vec{q}|$ small and assuming spherical symmetry, then

$$\begin{aligned} F(\mathbf{q}) &= \int d^3x\rho(\vec{x})\left(1+i\vec{q}\cdot\vec{x}-\frac{(\vec{q}\cdot\vec{x})^2}{2}+\mathcal{O}\left(\vec{q}^3\right)\right) \\ &= 1-\frac{1}{6}|\vec{q}|^2\left\langle r^2\right\rangle+\mathcal{O}\left(\vec{q}^4\right). \end{aligned} \tag{3.32}$$

From (3.32), one can see that the form factor gives access to the mean square radius :

$$r=-6\frac{\mathrm{d}F}{\mathrm{d}|\vec{q}|^2}\bigg|_{|\vec{q}|^2=0} \tag{3.33}$$

The same idea of form factors exists when the scattering is with the proton but it is more complicated, as the proton also possesses magnetic moment.

We introduce the four vector Γ^μ_{em}

$$\left\langle N\left(p'\right)\left|J^\mu_{em}(0)\right|N(p)\right\rangle=\bar{u}\left(p'\right)\Gamma^\mu_{em}u(p) \tag{3.34}$$

The most general form involving only p, p', γ^μ and respecting parity (no $\epsilon^{\mu\nu\rho\sigma}$ term) and relativistic invariance is

$$\Gamma^\mu_{em}=A\gamma^\mu+B(p^{\mu\prime}+p^\mu)+C(p^{\mu\prime}-p^\mu). \tag{3.35}$$

As Γ^μ_{em} is contracted to spinor fields, we can suppose that A, B, C is a function of a scale only, which is here then q^2. By current conservation, one finds that $C=0$

Using the Gordon identity

$$\bar{u}^{(\alpha)}\left(p'\right)\gamma^\mu u^{(\beta)}(p)=\frac{1}{2m}\bar{u}^{(\alpha)}\left(p^{\cdot rime}\right)\left[\left(p'+p\right)^\mu+i\sigma^{\mu\nu}\left(p'-p\right)_\nu\right]u^{(\beta)}(p) \tag{3.36}$$

gives the final form below for the four-vector:

$$\Gamma^\mu_{em}=\left[\gamma_\mu F_1\left(q^2\right)+i\sigma^{\mu\nu}q_\nu\frac{\kappa}{2M}F_2\left(q^2\right)\right], \tag{3.37}$$

where F_1, F_2 are real functions in the region $q^2<0$. They are called respectively the Dirac and Pauli form factors. κ is called the anomalous magnetic moment.

By definition, Γ^μ appears when one tries to calculate the scattering of the particle to an electromagnetic field A_μ. The leading order term in the scattering amplitude has the form $i\mathcal{M}\propto -ie(\bar{u}\Gamma^\mu u)A_\mu(q)$. One then considers the limit where $A_\mu=(\phi,\vec{0})$ is an classical electrostatic field, so $q^0=0$ and has with slow spatial variation so it is concentrated around $\vec{q}=0$. In this case, we have

$$i\mathcal{M}\propto -ie\bar{u}\gamma^0F_1(0)u\phi(q)\propto -i\tilde{V}(q)\bar{u}\gamma^0u$$

where $\tilde{V}(q)=\mathcal{Q}|e|\phi(q)$ and Q the charge of the particle unit of |e| , i.e. the scattering approaches to the one on a coulombic potential Therefore, this shows that $F_1(0)=\mathcal{Q}$. This remains true at all order.

Similarly, by considering the coupling with a slowly varying magnetostatic field, one shows that

$$g=2\left[F_1(0)+\kappa F_2(0)\right]=2\mathcal{Q}+2\kappa, \tag{3.38}$$

where g is the Landé factor. We normalise $F_2(0)=1$. The second term comes from radiative corrections. If $\kappa << 1$ and $g\simeq 2\mathcal{Q}$, the particle can be considered point-like, which is the case for electron or muon.

Howerver, experimental measurements have shown that the value for anomalous magnetic moment of the proton and neutron are $\kappa_p \simeq 1.7928$ and $\kappa_n \simeq -1.9130$, hence, confirming that nucleon have an inner structure.

3.2.2 Sachs electric and magnetic form factor

In practice, it is more physically meaningful and easier, as we will see later, to work with the Sachs electric and magnetic form factors defined by

$$\begin{aligned} G_E &\equiv F_1 + \frac{\kappa q^2}{4M^2} F_2 \\ G_M &\equiv F_1 + \kappa F_2 \end{aligned} \tag{3.39}$$

The physical significance is best understood in the Breit frame, corresponding to the center of mass frame for the incoming and outgoing proton. As $\vec{p} + \vec{p'} = 0$, then $q^0 = 0$. The four components for the hadronic current in this specific frame are

$$J^0 = eG_E(q^2) \tag{3.40}$$

$$\vec{J} = ieG_M(q^2)(\vec{\sigma} \times \vec{q})/M. \tag{3.41}$$

By comparison with the non-relativistic theory, we can then associate G_E and G_M to the Fourier transform of the electric charge and magnetic moment distribution [22].

Hence, the extraction of G_E and G_M from cross-section allows us to access the mean square radius of the charge and magnetic distribution as (3.32) suggested:

$$< r_E^2 >= 6 \frac{\mathrm{d}G_E}{\mathrm{d}q^2}\Big|_{q^2=0} \tag{3.42}$$

$$< r_M^2 >= 6 \frac{\mathrm{d}G_M}{\mathrm{d}q^2}\Big|_{q^2=0}. \tag{3.43}$$

In the laboratory frame, the approximation of G_E and G_M to the Fourier transform of charge density is valid as long as $|\vec{q}|^2 << M^2$.

Finally, we have at $Q^2 = 0$, the Sachs electric and magnetic form factors become:

$$G_E(0) = \mathcal{Q} \quad \text{et} \quad G_M(0) = \frac{\mu}{\mu_N} = \mathcal{Q} + \kappa \quad \text{with} \quad \kappa << 1 \tag{3.44}$$

where $\mu_N = \frac{|e|\hbar}{2M}$ is the nuclear magneton.

3.2.3 Hadronic current and spin

We note $P_\mu = p'_\mu + p_\mu$ and $P^2 = 4M^2 - q^2$. From the previous parts, Γ^μ_{em} for spin $1/2$ has the form (3.37).

Using the Gordon identity, Γ_μ can be rewritten as

$$\Gamma^\mu_{em} = -\frac{\kappa F_2}{2M} P^\mu + G_M \gamma^\mu \tag{3.45}$$

$$= \frac{F_1}{2M} P^\mu + i \frac{G_M}{2M} \sigma^{\mu\nu} q_\nu. \tag{3.46}$$

$$\tag{3.47}$$

In the point-like case, Γ^{μ}_{em} becomes

$$\Gamma^{\mu}_{em} = \mathcal{Q}\gamma^{\mu} = \frac{\mathcal{Q}}{2M}P^{\mu} + i\frac{\mathcal{Q}+\kappa}{2M}\sigma^{\mu\nu}q_{\nu}. \tag{3.48}$$

In the case of spin-0 particle, the matrix element takes the form

$$\left\langle m\left(p'\right)\left|J^{\mu}_{em}(0)\right|m(p)\right\rangle = P^{\mu}F, \tag{3.49}$$

where F satisfies $F(0) = \mathcal{Q}$. This reduces for point-like particle to

$$\left\langle m\left(p'\right)\left|J^{\mu}_{em}(0)\right|m(p)\right\rangle = \mathcal{Q}P^{\mu}. \tag{3.50}$$

.

3.2.4 Structure function in the elastic region

In the elastic case, the energy of the outgoing electron E' is fixed completely by the scattering angle θ and the energy of the incoming electron E. More precisely, the elastic relation $p'^2 = W^2 = (p+q)^2 = M^2$ gives

$$2p\cdot q + q^2 = 0 \quad \text{or in the laboratory frame} \quad M\left(E-E'\right) = 2EE'\sin^2\frac{\theta}{2}. \tag{3.51}$$

Thus, E' is fixed through the relation

$$E' = E\frac{1}{1+2\frac{E}{M}\sin^2\frac{\theta}{2}}, \tag{3.52}$$

where $\frac{1}{1+\frac{2E}{M}\sin^2\frac{\theta}{2}}$ corresponds to the recoil factor.

The expression of the elastic hadronic tensor from (3.15) has the form

$$W^{el}_{\mu\nu} = \frac{1}{4M^2}\delta\left(\nu + \frac{q^2}{2M}\right)H^{\mu\nu}_{el}, \tag{3.53}$$

where

$$H^{el}_{\mu\nu} = \frac{1}{2}\sum_{\sigma}\left\langle p,\sigma\left|J^{em}_{\mu}\right|p'\right\rangle\left\langle p'\left|J^{em}_{\nu}\right|p,\sigma\right\rangle. \tag{3.54}$$

To compute this, one need first to integrate over the phase-space of the outgoing proton. Then, the property $\delta\left(f(x)-f(x_0)\right) = \left(\frac{1}{|f'(x_0)|}\right)\delta\left(x-x_0\right)$ can be used twice here to obtain the delta function in (3.53). In more details, we have

$$\begin{aligned}
\delta\left(p'_0 - M - q_0\right) &= \delta\left[p'_0\left(E'\right) + E' - (M+E)\right] \\
&= \left|\frac{d\left(p'_0\left(E'\right)+E'\right)}{dE'}\right|^{-1}\delta\left[E' - E'(E,\theta)\right] \\
&= \left|\frac{ME}{p'_0E'}\right|^{-1}\delta\left[E' - E'(E,\theta)\right].
\end{aligned} \tag{3.55}$$

In the same way,

$$\begin{aligned}
\delta\left(\nu + \frac{q^2}{2M}\right) &= \delta\left(E - E' - \frac{2EE'}{M}\sin^2\frac{\theta}{2}\right) \\
&= \left|\frac{\partial\left(\nu+\frac{q^2}{2M}\right)}{\partial E'}\right|^{-1}\delta\left[E' - E'(E,\theta)\right] \\
&= \frac{E'}{E}\delta\left[E' - E'(E,\theta)\right].
\end{aligned} \tag{3.56}$$

We now compute $H^{el}_{\mu\nu}$. The simplest way to do so is to use for the current matrix element, the expression given by (3.45):

$$\begin{aligned} H^{\mu\nu}_{el} &= \frac{1}{2}\,\mathrm{Tr}\left[\left(\not{p}' + M\right)\left(-\frac{\kappa F_2}{2M}P_\mu + G_M\gamma^\mu\right)\left(\not{p} + M\right)\left(-\frac{\kappa F_2}{2M}P_\nu + G_M\gamma^\nu\right)\right] \\ &= -\kappa F_2\left(G_E + G_M\right)\left(4M^2 - q^2\right)P_\mu P_\nu + G_M^2 h_{\mu\nu}, \end{aligned} \tag{3.57}$$

where

$$h_{\mu\nu} = 2\left(p_\mu p'_\nu + p'_\mu p_\nu + \frac{q^2}{2}g_{\mu\nu}\right). \tag{3.58}$$

In the point-like case, $H^{\mu\nu}_{el}$ reduces to

$$H^{\mu\nu}_{el} = \mathcal{Q}^2 h^{\mu\nu}. \tag{3.59}$$

. The elastic differential cross-section, obtained after integration over E' of (3.29), reads

$$\frac{d^2\sigma^{el}}{d\Omega} = \frac{\alpha^2}{q^4}\frac{E'^2}{E^2}\ell^{\mu\nu}H^{el}_{\mu\nu}. \tag{3.60}$$

We have then something similar in terms of cross-section as for electron-muon process if $h_{\mu\nu}$ is considered the analogue to the muon leptonic tensor but for point-like hadrons.

Projecting $H^{\mu\nu}_{el}$ using P^μ_L and $g^{\mu\nu}_\perp$, defined by (3.23) and (3.24), leads to the expression of the elastic structure functions

$$\begin{aligned} W^{el}_1 &= -\frac{q^2}{4M^2}G_M^2\,\delta\left(\nu + \frac{q^2}{2M}\right) \\ W^{el}_2 &= \frac{G_E^2 - \frac{q^2}{4M^2}G_M^2}{1 - \frac{q^2}{4M^2}}\,\delta\left(\nu + \frac{q^2}{2M}\right), \end{aligned} \tag{3.61}$$

which become for one-point particle:

$$\begin{aligned} W^{el}_{1pt} &= -\frac{q^2}{4M^2}\mathcal{Q}^2\,\delta\left(\nu + \frac{q^2}{2M}\right) \\ W^{el}_{2pt} &= \mathcal{Q}^2\,\delta\left(\nu + \frac{q^2}{2M}\right). \end{aligned} \tag{3.62}$$

3.2.5 The elastic differential cross-section

Finally, the differential cross-section for the electron-nucleon in the elastic regime has the form

$$\frac{d\sigma^{el}}{d\Omega} = \frac{\alpha^2}{4E^2\sin^4\frac{\theta}{2}}\frac{1}{1 + \frac{2E}{M}\sin^2\frac{\theta}{2}}\left\{\frac{Q^2}{2M^2}G_M^2\sin^2\frac{\theta}{2} + \frac{G_E^2 + \frac{Q^2}{4M^2}G_M^2}{1 + \frac{Q^2}{4M^2}}\cos^2\frac{\theta}{2}\right\}. \tag{3.63}$$

This is the Rosenbluth formula.

We see then that there is interference between the Dirac and Pauli form factors so their errors on their measurement are higher and more correlated compared to Sachs form factor. This is one of the reason why they have been defined.

In the point-like limit, this becomes

$$\left(\frac{d\sigma^{el}}{d\Omega}\right)_{pt} = \frac{\mathcal{Q}^2\alpha^2}{4E^2\sin^4\frac{\theta}{2}}\frac{1}{1 + \frac{2E}{M}\sin^2\frac{\theta}{2}}\left\{\frac{Q^2}{2M^2}\sin^2\frac{\theta}{2} + \cos^2\frac{\theta}{2}\right\}. \tag{3.64}$$

In the Mott regime where $Q^2 << M^2$ or equivalently $E - E' << M^2$, it reduces to

$$\left(\frac{d\sigma}{d\Omega}\right)_{Mott} = \frac{1}{1 + \frac{2E}{M}\sin^2\frac{\theta}{2}} \frac{\mathcal{Q}^2\alpha^2\cos^2\frac{\theta}{2}}{4E^2\sin^4\frac{\theta}{2}}. \tag{3.65}$$

Therefore,

$$\frac{d\sigma^{el}}{d\Omega} = \left(\frac{d\sigma}{d\Omega}\right)_{Mott} \left[\frac{G_E^2 + \tau G_M^2}{1+\tau} + 2\tau G_M^2 \tan^2\frac{\theta}{2}\right] \frac{1}{\mathcal{Q}^2} \tag{3.66}$$

with $\tau = \frac{Q^2}{4M^2}$.

3.2.6 Phenomenology

One method to extract G_E and G_M is the Rosenbluth separation method. It consists in measuring the differential cross-section for different values of θ at fixed Q^2. In the early use of this method, some kind of reduced differential cross-section were defined and analyzed which are dependent on the diffusion angle. As an example, in [21], they define $R(\theta, q^2) = \cot^2\frac{\theta}{2}\left[G_E^2 + \tau G_M^2\right] + \tau\left(1+\tau\right)G_M^2$ and plot it as a function of q^2.

The modern notation of the elastic cross-section is

$$\frac{\mathrm{d}\sigma}{\mathrm{d}\Omega} = \left(\frac{\mathrm{d}\sigma}{\mathrm{d}\Omega}\right)_{Mott} \frac{1}{1+\tau}\left[G_E^2 + \frac{\tau}{\epsilon}G_M^2\right]\frac{1}{\mathcal{Q}^2}, \tag{3.67}$$

where $\epsilon = \left[1 + 2(1+\tau)\tan^2\frac{\theta}{2}\right]^{-1}$ is the virtual photon polarization.

Thus, one makes use of the linear dependence on ϵ and defines the reduced cross-section

$$\left(\frac{d\sigma}{d\Omega}\right)_{\text{reduced}} = \frac{\epsilon(1+\tau)}{\tau}\left(\frac{d\sigma}{d\Omega}\right)_{\text{exp}} / \left(\frac{d\sigma}{d\Omega}\right)_{\text{Mott}} = G_M^2 + \frac{\epsilon}{\tau}G_E^2. \tag{3.68}$$

Plotting this reduced differential cross-section as a function of ϵ for fixed Q^2 gives G_E^2 as the slot and G_M^2 as the ordinate intercept.

Using (3.42), one finds $r_E \sim 0.8fm$.

Moreover, as shown by figure 3.2, for $Q^2 \geqslant M^2$, with $M^2 \sim 1\text{GeV}$, the precision on the measure of G_E strongly decreases. This is due to the presence of factor of $\frac{1}{1+\tau}$ that multiplies G_E^2. For $Q^2 \leqslant 1\text{GeV}$, we have $G_{E_p} \sim G_D$ where

$$G_D = \frac{1}{\left(1 - \frac{q^2}{0.7\text{GeV}}\right)^2} \tag{3.69}$$

is the dipole form factor. By contrast, from figure 3.3, one can see that $G_{M_p} \sim \mu_p G_D$ is accurate for large Q^2.

Another method used to extract form factors is with the double polarization technique. One either have the incoming electron beam and target that are polarized or uses the recoil polarization technique. In this latter case, the recoiled proton is polarized by the the incoming beam. Its polarization is measured giving P_ℓ, longitudinal component, parallel to its momentum and P_t, transverse component, orthogonal to its momentum. The ratio $\frac{G_E}{G_M}$ is related to them through

$$\frac{G_E}{G_M} = -\frac{P_t}{P_\ell}\frac{E+E'}{2M}\tan\frac{\theta}{2}. \tag{3.70}$$

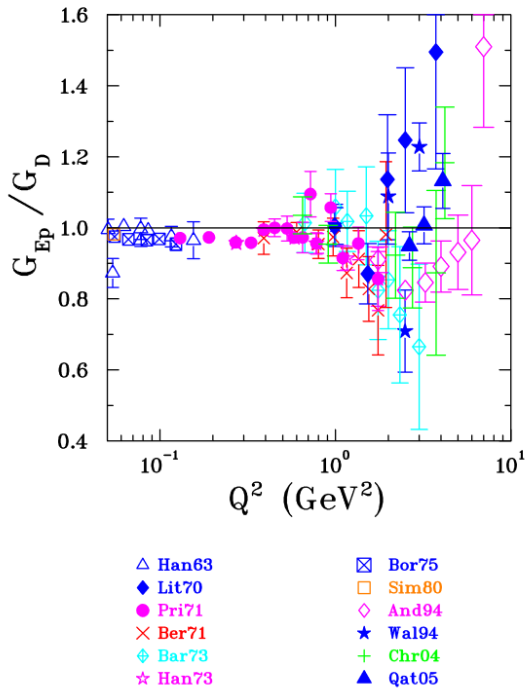

Figure 3.2: Data for G_{E_p} using the Rosenbluth separation. From [30] based on [21], [27], [35],[6], [4], [24], [9], [40],[2], [10],[43],[12],[36]

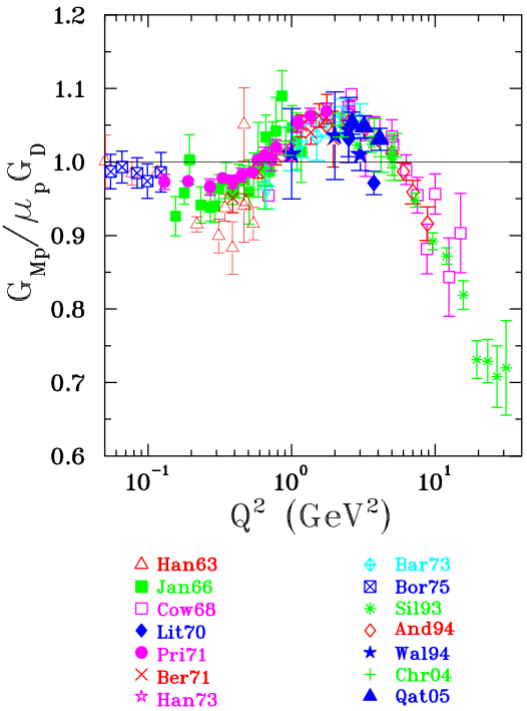

Figure 3.3: Data for G_{M_p} using the Rosenbluth separation. From [30] based on [21], [27], [35],[6], [4], [24], [9],[2],[10],[43],[12],[36],[26],[13],[39]

From 3.4, one can see that the scaling law $G_{E_p} \sim \frac{G_{M_p}}{\mu_p}$ do not survive. It is now assumed that the discrepancies between results using the Rosenbluth separation method or polarization technique are due to the fact that radiative corrections have not been taken into account in the cross-section. In fact, all the analysis so far has been done at Born level but the exchange of two virtual photons can also be

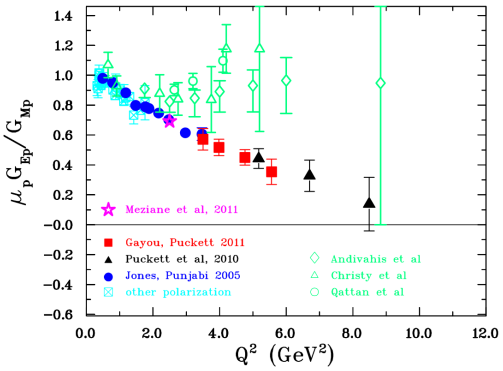

Figure 3.4: Data from the three G_{E_p} experiments at JLab based on recoil polarization technique[31]

considered. Nevertheless, the effect of taking into account two photons effect are not apparent in polarization experiments. Its contribution to $e^- p \to e^- p$ is yet to be determined.

3.2.7 Asymptotic behaviour of form factors

In the region of deep elastic scattering i.e. $x_{Bj} < 1$ and Q^2 large $Q^2 >> \lambda^2_{QCD}$, one can use perturbative QCD to predict the dominant power contribution to the asymptotic behaviour of the form factors using hard counting rules[11]. The asymptotic behaviour are derived in the context of the parton model and rely on dimensional analysis. A proper justification of these rules are based on factorisation theorem which allows us to separate the hard part corresponding to short distance dynamics from the soft part corresponding to long distance dynamics.

The leading order diagram is illustrated in Figure 3.5.

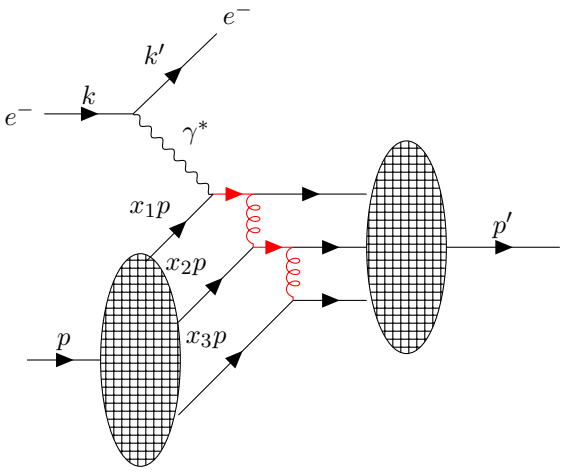

Figure 3.5: Deep elastic scattering in the parton model. The blob correspond to the soft part. In red are the hard propagators.

The analysis of the hard scale is made in the Breit frame, where $\vec{p'} + \vec{p} = 0$ giving then $\vec{q} = -2\vec{p}$. In this specific frame, the transverse momentum of the partons can be neglected.Therefore, their momentum have approximately the form $p_i = x_i p$ where x_i is the fraction of the proton momentum carried by the parton i $(\sum_i x_i = 1)$.

The hard counting rules are listed below.

- Hard gluons exchange should happen to ensure the elasticity of the scattering, meaning the non-fragmentation of the proton due to the high momentum transfer from the photon. The contribution of each gluon propagator is of order $\frac{1}{Q^2}$.
- The contribution for the fermionic propagator is of order $\frac{1}{Q}$.
- In the short distance dynamics, the partons are considered as free. Hence, the incoming and outgoing fermions can be replaced by free spinors $u \sim \sqrt{2E}\xi \sim \sqrt{2x_i|\vec{p}|}\xi \sim \sqrt{Q}\xi$ where ξ are elementary spinors.

Thus, the matrix element of the partonic electromagnetic current has the asymptotic behaviour

$$\begin{aligned} \left|\left\langle N\left(p'\right)\left|J_\mu\right|N(p)\right\rangle\right| &\sim A\left(\frac{1}{Q^2}\right)^2\left(\frac{1}{Q}\right)^2\left(\sqrt{Q}\right)^6 \\ &\sim \frac{A}{Q^3}, \end{aligned} \tag{3.71}$$

where A is a constant. From (3.37), this gives us

$$\frac{A}{Q^3} \sim \left|\bar{u}'\gamma_\mu u F_1\right|. \tag{3.72}$$

A factor of Q relates F_1 and the amplitude.

$$\begin{aligned} &F_1\left(Q^2\right) \simeq \tfrac{1}{Q^4} \\ &F_2\left(Q^2\right) \simeq \tfrac{1}{Q^6} \\ &G_E \sim G_M \sim \tfrac{1}{Q^4} \end{aligned} \quad , \tag{3.73}$$

where F_2 comes from $\frac{A}{Q^3} \sim |\bar{u}'\sigma_{\mu\nu}uq_\nu F_2|$.

This can be generalized. For a hadron with n constituents in the quark model i.e. $n = 2$ for a meson and $n = 3$ for a baryon, the form factor has the following behaviour,

$$F_n\left(q^2\right) \simeq \frac{C}{\left(Q^2\right)^{n-1}}. \tag{3.74}$$

Another formalism used to determine the behaviour of form factors is by working in the Sudakov frame. First, let's define the light cone variables. If $\left(v^0, v^1, v^2, v^3\right)$ is an arbitrary vector, the light-cone variables are defined as

$$\begin{aligned} v^\pm &= \frac{1}{\sqrt{2}}\left(v^0 \pm v^3\right) \\ \underline{v} &= v_T = \left(v^2, v^3\right) = -v_\perp \quad \text{euclidian metric for} \underline{v}\text{`} \end{aligned} \quad . \tag{3.75}$$

The scalar product in this basis is $v_1 \cdot v_2 = v_1^+ v_2^- + v_1^- v_2^+ - \underline{v_1} \cdot \underline{v_2}$.

In Sudakov frame, two light-cone vectors p_1, p_2 are defined, going in + and - directions. We note $2p_1 \cdot_2 = s$. Here, we can choose $p_1 = p$ and $p_2 = p$ giving then sQ^2. All other vectors are then expressed in term of those two vectors:

$$\begin{array}{cccc} k & = \alpha p_1 + & \beta p_2 + & k_\perp \\ & + & - & \perp \end{array} . \tag{3.76}$$

Its square reads

$$k^2 = \alpha\beta s + k_\perp^2 = \alpha\beta s - \underline{k}^2 = 2k^+k^- - \underline{k}^2. \tag{3.77}$$

The decomposition of the elastic scattering in this frame is schematically represented in figure 3.6. We observe a necessary flip of both directions in the hard part. One can show that $\alpha\beta s$ is of order Q^2. Hence, one recovers the same contribution for propagators in the hard part as with the hard counting rules. Thus, the hard part is of order $\left(\frac{1}{Q^2}\right)^2 \left(\frac{1}{Q}\right) \frac{1}{Q^6}$. The form factor F_2 associated with this flip is then $\sim \frac{1}{Q^6}$.

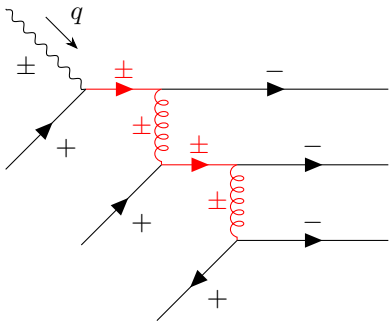

Figure 3.6: Hard part of e-p elastic scattering in the Sudakov frame. The hard propagators are represented in red

Unfortunately, the experimental data found at SLAC and JLab are not in agreement with the perturbative QCD prediction (3.73). The scaling law $\frac{Q^2 F_2(Q^2)}{F_1(Q^2)}$ can be improved if the parton orbital angular momentum are taken into account [5]. The scaling law obtained is $\frac{Q^2 F_2(Q^2)}{F_1(Q^2)} \sim \ln^2\left(\frac{Q^2}{\lambda^2}\right)$ and seems to better agree with experimental results.

3.3 Deep inelastic scattering

The core statement in the parton model for deep inelastic scattering is that the electron scatters elastically to a parton, considered as free, instead of the whole proton. The deep inelastic scattering is then illustrated by figure 3.7.

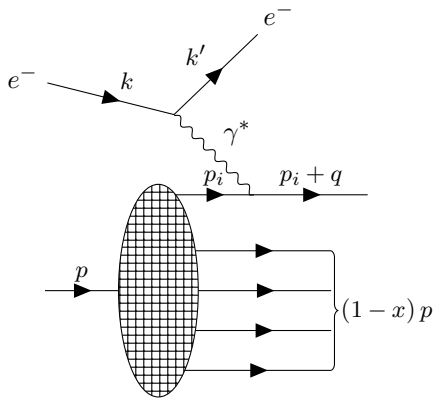

Figure 3.7: $e^- p$ deep inelastic scattering in the parton model

The kinematics used have already been described in 3.1.1.

3.4 The parton model and the impulse approximation

Drell et Yan [15] argued that the parton model is the application of the impulse approximation to high energy particle physics and justify this approximation using a frame where the longitudinal momentum of the proton is large $P^2 >> M^2$, called infinite momentum frame and when one works in the Bjorken limit, $Q^2 \to \infty, \nu \to \infty$ and x_{Bj} is fixed and finite.

3.4.1 The impulse approximation and validity

The impulse approximation is a concept that lies within low energy atomic and nuclei physics. In the case of a one-particle projectile that scatters to a target in a bound state, the approximation is that the scattering is between the projectile and one particle of the target, considered as free. This relies upon some assumptions, notably that the range of interaction is small compared to the inter-distances inside the target and that the interaction time is small enough to ignore the binding energy inside the target.

In the regime of deep scattering, the wave length of the virtual photon is of order $\frac{1}{Q}$. For Q^2 sufficiently large then, it is much consequently much smaller than the radius of the proton: $r_p \simeq 1\text{fm}$. The first condition for the approximation is then respected.

We will now consider the two time scales of interest in DIS. If we note by x the fraction of longitudinal momentum of the parton that interacts with the virtual photon, $p_{1\perp}$, m_1 and $p_{2\perp}$, m_2 being the transverse momentum and masses of the parton and of the rest of the constituents in the proton, then the interaction time is of order :

$$T \sim \frac{1}{\Delta E} \sim \frac{1}{\sqrt{(xP)^2 + p_{1\perp}^2 + m_1^2} + \sqrt{((1-x)P)^2 + p_{2\perp}^2 + m_2^2} - \sqrt{P^2 + M^2}} \tag{3.78}$$

$$\underset{P\to\infty}{\overset{P\to\infty}{\sim}} \frac{1}{2\left(|x| + |1-x| - 1\right)P^2 + \frac{p_{1\perp}^2 + m_1^2}{x} + \frac{p_{2\perp}^2 + m_2^2}{1-x} - M^2} \tag{3.79}$$

$$\sim \frac{2P}{\frac{m_1^2 + p_{1\perp}^2}{x} + \frac{m_2^2 + p_{2\perp}^2}{1-x} - M^2} \quad \text{for} \quad 0 < x < 1 \tag{3.80}$$

$$\sim \frac{2P}{M_{eff}^2} \tag{3.81}$$

The time of the interaction in the center-of-mass frame, which is a particular example of infinite momentum frame has the form:

$$\tau \sim \frac{1}{q^0} = \frac{4P}{2M\nu - Q^2} \tag{3.82}$$

In order to have $\tau << T$, the condition $M_{eff}^2 << 2M\nu - Q^2$ should be respected. This requires to have $p_{i\perp}$ bounded and x away from its end points. The Bjorken limit ensures the later, as one can easily prove that, in the naive parton model, $x = s_{Bj}$ from the elasticity condition : $(p_i + q)^0 :\simeq 0$. For the former, transverse motion are caused by strong interaction and therefore the transverse momentum is in the order of the binding energy, which itself is of order the mass, and so in an infinite momentum frame where $P^2 >> M^2$, the transverse momentum is negligible : $p_{i\mu} \simeq x p_\mu$

Hence, the time scales are such that the binding forces are negligible during the time of the electromag-

netic interaction.

Since the impulse approximation ca nbe applied, one can therefore factorize between the hard part and non-perturbative soft part:

$$\frac{\mathrm{d}\sigma}{\mathrm{d}t}\left(e^- p \to e^- p\right) = \sum_i \int \mathrm{d}x\, f_i(x) \frac{\mathrm{d}\hat{\sigma}}{\mathrm{d}t}\left(e^- q_i \to e^- q_i\right) \tag{3.83}$$

where $f_i(x)dx$ is the probability that the parton q_i interacting with the photon has its longitudinal momentum fraction between x and $x + \mathrm{d}x$. $f_i(x)$ is called the parton distribution functions and are supposed to be universal, process-independent.

We note that struck parton cannot go backward i.e. has $x < 0$ or $x > 1$. If that was the case, the transition amplitude of going from a proton state to a parton and its other constituents (which has the same form as T) would have a factor of P^2 in its denominator, as one can see from (3.79). Hence, the probability to have a backward parton is very much suppressed.

3.4.2 Infinite momentum frames

A whole family of infinite momentum frame exists but not all of them are convenient in treating DIS in the parton model and interpreting the results.

Listed below are some common frames used to discuss the parton model.

First, the four-momentum of the proton is chosen as

$$p_\mu = \left(\sqrt{P^2 + M^2}, 0_\perp, P\right) \sim_{P\to\infty} \left(P + \frac{M^2}{2P}, 0_\perp, P\right) \tag{3.84}$$

The constraints on $q_\mu = (q_0, q_\perp, q_z)$ are

$$p \cdot q = M\nu \simeq P\left(q_0 - q_z\right) + \frac{M^2}{2P} q_0, \quad q^2 = \left(q_0 - q_z\right)\left(q_0 + q_z\right) - \underline{q}^2 \tag{3.85}$$

The parametrisation

$$q_0 - q_z = \frac{A}{P}$$
$$q_0 = BP$$

enables us to have $M\nu$ and Q^2 independent of P in the limit case where $P \to \infty$.

Different choices of A and B give different infinite momentum frame. The two extreme cases are :

1. For $A = 0 \quad B = \frac{2\nu}{M}$;

$$q_\mu = \left(\frac{2\nu}{M} P, q_\perp, \frac{2\nu}{M} P\right) \quad \text{with} \quad q^2 = q_\perp^2 = -\underline{q}^2$$

   This is the case where $q_0 = q_z \sim P$.

2. For $A = M\nu \quad B = \frac{2M\nu + q^2}{4P^2}$;

$$q = \left(\frac{2M\nu + q^2}{4P}, q_\perp, \frac{q^2 - 2M\nu}{4P}\right)$$

   It corresponds to the extreme case $q_0 \sim q_z \sim \frac{1}{P}$. One can check that it is the center-of-mass frame.

3. $B = \frac{M\nu}{P^2}, A = M\nu$:

$$q = \left(\frac{M\nu}{P}, q_\perp, 0\right) = \left(\frac{Q^2}{2x_{Bj}P}, q_\perp, 0\right) \simeq (0, q_\perp, 0)$$

As for the one above, it also corresponds to small q_0 and q_z. This is called the Bjorken frame.

4. $A = \frac{Q^2}{2x_{Bj}}$ and $B = -x_{Bj} + \frac{Q^2}{4x_{Bj}P^2}$;
This choice gives the Sudakov frame, which is introduced in 3.2.7. The idea behind this frame is to define the two light-like basis vectors p_1 and p_2 such that, for processes with two massless colliding particles, the two projectiles have their momentum along the two light cones directions +/-.
Setting $p_1 = P\,(1, 0_\perp, -1) \quad p_2 = \frac{p\cdot q}{2P}\,(1, 0_\perp, 1)$ gives, for $Q^2 >> M^2$,

$$p = p_2, \quad q = p_1 - x_{Bj}p_2, \quad p_1^2 = p_2^2 = 0 \quad \text{and} \quad p_1 \cdot p_2 = p \cdot q$$

The Breit frame is also an infinite momentum frame, where the momentum of the incoming parton is reversed after scattering:

$$q = (0, 0_\perp, -2x_{Bj}P) = (0, 0_\perp, -Q)\,, \quad p_i = xp = (xP, 0_\perp, xP)\,, \quad p_i + q = xp + q = (xP, 0_\perp, -xP)$$

Lastly, another frame of interest is the referential frame of the proton :

$$q = \left(\nu, 0_\perp, \sqrt{Q^2 + \nu^2}\right) \overset{\nu^2 >> Q^2}{\simeq} \left(\nu, 0_\perp, \nu + \frac{Q^2}{2\nu}\right) = \left(\frac{Q^2}{2x_{Bj}M}, 0_\perp, \frac{Q^2}{2x_{Bj}M} + Mx_{Bj}\right)$$

.

It is an infinite momentum frame from the point of view of the virtual photon.

3.5 Consequences of the parton model on structure functions

We introduce new structure functions :

$$\begin{aligned} \lim_{\substack{q^2\to\infty \\ x_{Bj}\text{fixed}}} MW_1\left(q^2, \nu\right) &= F_1\left(x_{Bj}, Q^2\right) \\ \lim_{\substack{q^2\to\infty \\ x_{Bj}\text{fixed}}} \nu W_2\left(q^2, \nu\right) &= F_2\left(x_{Bj}, Q^2\right) \end{aligned} \tag{3.86}$$

In this naive parton model, the electron scatters elastically to a "free" parton. Hence, for a proton composed of a parton of mass m and charge $\mathcal{Q}$, then from from their expression in the elastic regime, its structure functions has the form

$$W_1(\nu, Q^2) = \frac{\mathcal{Q}^2}{4m^2}\delta\left(\nu - \frac{Q^2}{2m}\right) = \frac{\mathcal{Q}^2}{4m^2\nu}\delta\left(1 - \frac{Q^2}{2m\nu}\right) \tag{3.87}$$

$$W_2(\nu, Q^2) = \delta\left(\nu - \frac{Q^2}{2m}\right) = \frac{1}{\nu}\delta\left(1 - \frac{Q^2}{2m\nu}\right) \tag{3.88}$$

Neglecting transverse momentum gives $p_{i\mu} = xp_\mu$, hence $m = xM$ [1]. Thus,

$$\begin{aligned} F_1 &= \frac{\mathcal{Q}^2}{4Mx^2\nu}\delta\left(1 - \frac{Q^2}{2Mx\nu}\right) = \frac{x_{Bj}}{2x}\delta\left(x_{Bj} - x\right) \\ F_2 &= \delta\left(1 - \frac{Q^2}{2Mx\nu}\right) = x\delta\left(x_{Bj} - x\right) \end{aligned} \tag{3.89}$$

Finally, as protons have all type of partons i with charge e_i in units of $|e|$, the proton structure functions are obtained by weighing the above functions with $f_i(x)dx$, introduced in (3.83) and summed over i:

$$\begin{aligned} F_1\left(x_{Bj}\right) &= \sum_i \int \mathrm{d}x \;\; e_i^2 f_i(x) \frac{x_{Bj}}{2x}\delta\left(x_{Bj} - x\right) \\ F_2\left(x_{Bj}\right) &= \sum_i \int \mathrm{d}x \;\; e_i^2 f_i(x) x\delta\left(x_{Bj} - x\right) \end{aligned} \tag{3.90}$$

Two observations can be made on (3.90). First, F_1, F_2 only depend on x_{Bj} and not on Q^2. This is the Bjorken scaling[7]. This behaviour will not remain true once radiative corrections are included, as we will see in 3.8. The second observation is that they respect Callan-Gross relation

$$F_2\left(x_{Bj}\right) = 2x_{Bj}F_1\left(x_{Bj}\right) \tag{3.91}$$

This is a consequence of partons having spin $\frac{1}{2}$, as it was derived from their expressions in the elastic regime, structure function in elastic scattering of a point-like particle of spin $\frac{1}{2}$.

3.6 Tests of parton spin

3.6.1 Callan-Gross relation

An equivalent form of (3.91) exists, which is derived by comparing the differential cross-section of e^-p with $e^-\mu^-$. The Mandelstam variables for the partonic subprocess are :

$$\hat{s} = (k + p_i)^2 \simeq \hat{t} = \left(k - k'\right)^2 = -Q^2 \simeq -x_{Bj}yS\hat{u} = \left(k' - p_i\right)^2 = -\hat{s} - \hat{t} = -x_{Bj}\left(1 - y\right)S \tag{3.92}$$

where $S = (k + p)^2$ and electron and quark masses are neglected.

As parton are point-like and spin $\frac{1}{2}$, the differential cross-section of the subprocess e^-q_i is given by the one from $e^-\mu^-$:

$$\begin{aligned} \frac{\mathrm{d}\hat{\sigma}}{\mathrm{d}t} &= \frac{2\pi\alpha^2 e_i^2}{\hat{s}^2}\frac{\hat{s}^2 + (\hat{s} + \hat{t})^2}{\hat{t}^2} \\ &= \frac{2\pi\alpha^2 e_i^2}{Q^4}\left[1 + (1 - y)^2\right] \end{aligned} \tag{3.93}$$

Therefore, from (3.83), the differential cross-section reads

$$\frac{\mathrm{d}^2\sigma}{x_{Bj}dQ^2} = \frac{2\pi\alpha^2}{x_{Bj}Q^4}\left[1 + (1 - y)^2\right]F_2 \tag{3.94}$$

$1 + (1 - y)^2$ behaviour of the Cross-section is another proof of partons having spin 1/2.

[1] In reality, the partons cannot have mass $m = xM$. This would mean that quarks mass are not negligible compared to the proton mass. However, in an infinite momentum frame, as $P >> M$, then all masses are negligible.

This behaviour is found when comparing (3.94) with the general form of the differential cross-section (3.29), which can be rewritten into

$$\frac{d^2\sigma}{\bar{x}_{Bj}dy} = \frac{4\pi\alpha^2}{x_{Bj}yQ^2}\left[x_{Bj}y^2F_1 + \left(1 - y - x_{Bj}^2y^2\frac{M^2}{Q^2}\right)F_2\right] \tag{3.95}$$

We introduce the transverse and longitudinal structure functions associated to the cross-section $\gamma^*_{L/T}p \to X$, as we will see in the next paragraph:

$$\begin{aligned} F_T &= 2x_{Bj}F_1 \\ F_L &= F_2 - 2x_{Bj}F_1 \end{aligned} \tag{3.96}$$

Longitudinal polarisation cross-section has a significant contribution when

$$\frac{Q^2}{x_{Bj}^2} \simeq \frac{S}{x_{Bj}} \gg M^2 \quad \Rightarrow y \simeq \frac{Q^2}{x_{Bj}S} \quad \text{and} \quad \frac{\nu^2}{Q^2} = \frac{Q^2}{4M^2x_{Bj}^2} >> 1 \tag{3.97}$$

In this case,

$$\begin{aligned} \frac{\mathrm{d}^2\sigma}{\mathrm{d}x_{Bj}\,\mathrm{d}Q^2} &= \frac{y}{Q^2}\frac{\mathrm{d}^2\sigma}{\mathrm{d}x_{Bj}\,\mathrm{d}y} \\ &\simeq \frac{2\pi\alpha^2}{x_{Bj}yQ^2}\left\{\left[2(1-y)+y^2\right]F_2 - y^2F_L\right\} \end{aligned} . \tag{3.98}$$

Callan-Gross relation gives $F_L = 0$ and $F_T = F_2$. Therefore, (3.98) gives back (3.94) and both of them are proof of partons having spin $1/2$.

Callan-Gross is violated when taking into account QCD corrections.

3.6.2 R ratio

The expression of the total cross-section for the photo-absorption of the virtual photon has the form

$$\sigma^{\mathrm{tot}}\left(\gamma^*p \to X\right) = \frac{4\pi\alpha^2}{K_{\gamma^*}}W^{\mu\nu}\epsilon^*_\mu\epsilon_\nu \tag{3.99}$$

where $W^{\mu\nu}$ is the hadronic tensor and ϵ_μ vectors are defined in 3.1.3.

Two conventions exist for K_{γ^*} :

- Gilman :

$$K_{\gamma^*} = \nu + \frac{Q^2}{2\nu}$$

- Hand :

$$K_{\gamma^*} = \nu - \frac{Q^2}{2M}$$

Using the decomposition of $W^{\mu\nu}$ 3.27 with (3.97), one gets the cross-section for longitudinal and transverse polarized photon

$$\begin{aligned} \sigma_T \equiv \sigma^{tot}\left(\gamma^*_\perp p \to X\right) &= \frac{4\pi^2\alpha}{K_{\gamma^*}}\frac{F_T}{2Mx_{Bj}} \\ \sigma_L \equiv \sigma^{tot}\left(\gamma^*_L p \to X\right) &= \frac{4\pi^2\alpha}{K_{\gamma^*}}\frac{F_L}{2Mx_B} \end{aligned} \tag{3.100}$$

The ratio R is defined by

$$R \equiv \frac{\sigma_L}{\sigma_T} = \frac{F_L}{F_T} \tag{3.101}$$

Depending on the spin of the parton, R has different values :

- if all partons are spin $\frac{1}{2}$, $R \to 0$ as $F_L = 0$ from Callan-Gross relation
- if all partons have spin 0, $R \to \infty$. This is because for particle of spin 0, one can show that $F_1 = 0$.
- if there is a mix of partons of spin 0 and $1_{\overline{2, Tis finite}}$ Experiments at SLAC, where Q^2 ranged between 1.5 and 21 $(GeV/c)^2$, has found that $R \in [0; 0.5]$ [28].

3.7 The parton structure of nucleons

By isospin symmetry SU(2), we have :

$$\begin{aligned} f_u^{(p)} &= f_d^{(n)} \equiv u \\ f_d^{(p)} &= f_u^{(n)} \equiv d \\ f_s^{(p)} &= f_s^{(n)} \equiv s \end{aligned}$$

Moreover, the partons distribution function should respect the sum rules, corresponding to the conservation of quantum number :

- Charge conservation:

$$\begin{aligned} Q &= \int_0^1 dx \left[\frac{2}{3}(u - \bar{u}) - \frac{1}{3}(d - \bar{d})\right] = 1 \quad \text{for proton} \\ Q &= \int_0^1 dx \left[\frac{2}{3}(d - \bar{d}) - \frac{1}{3}(u - \bar{u})\right] = 0 \quad \text{for neutron} \end{aligned} \tag{3.102}$$

- Isospin number :

$$\begin{aligned} I_3 &= \frac{1}{2}\int_0^1 dx[(u - \bar{u}) - (d - \bar{d})] = \frac{1}{2} \quad \text{for proton} \\ I_3 &= \frac{1}{2}\int_0^1 dx[(d - \bar{d}) - (u - \bar{u})] = -\frac{1}{2} \quad \text{for neutron} \end{aligned} \tag{3.103}$$

- Strangeness :

$$S = \int_0^1 dx(s - \bar{s}) = 0 \tag{3.104}$$

- Baryonic number :

$$B = \frac{1}{3}\int [u - \bar{u} + d - \bar{d} + s - \bar{s}] = 1 \tag{3.105}$$

The sum rule on B can be obtained using the relation $Q = I_3 + \frac{Y}{2}$ with $Y = B + S$.

Combining the condition on Q for the proton and neutron, we get

$$\begin{aligned} \int_0^1 dx(u - \bar{u}) &= 2 \\ \int_0^1 dx(d - \bar{d}) &= 1 \end{aligned} \tag{3.106}$$

i.e. the net number of each type of quark is the number of quarks in the quark model.

Finally, the last sum rule to consider is energy-momentum conservation for proton and neutron:

$$\int_0^1 \mathrm{d}x\, x\left[u(x,Q^2)+d(x,Q^2)+s(x,Q^2)+\bar{u}(x,Q^2)+\bar{d}(x,Q^2)+\bar{s}(x,Q^2)+g(x,Q^2)\right]=1, \qquad (3.107)$$

where $g(x,Q^2)$ is the gluon distribution. Its presence is important as experimental data show that quarks carry only approximately $\sim 50\%$ of the total momentum of the proton [32].

Same kind of sum rules exist for the neutron.

The qualitative shape of F_2 is described in figure 3.8.

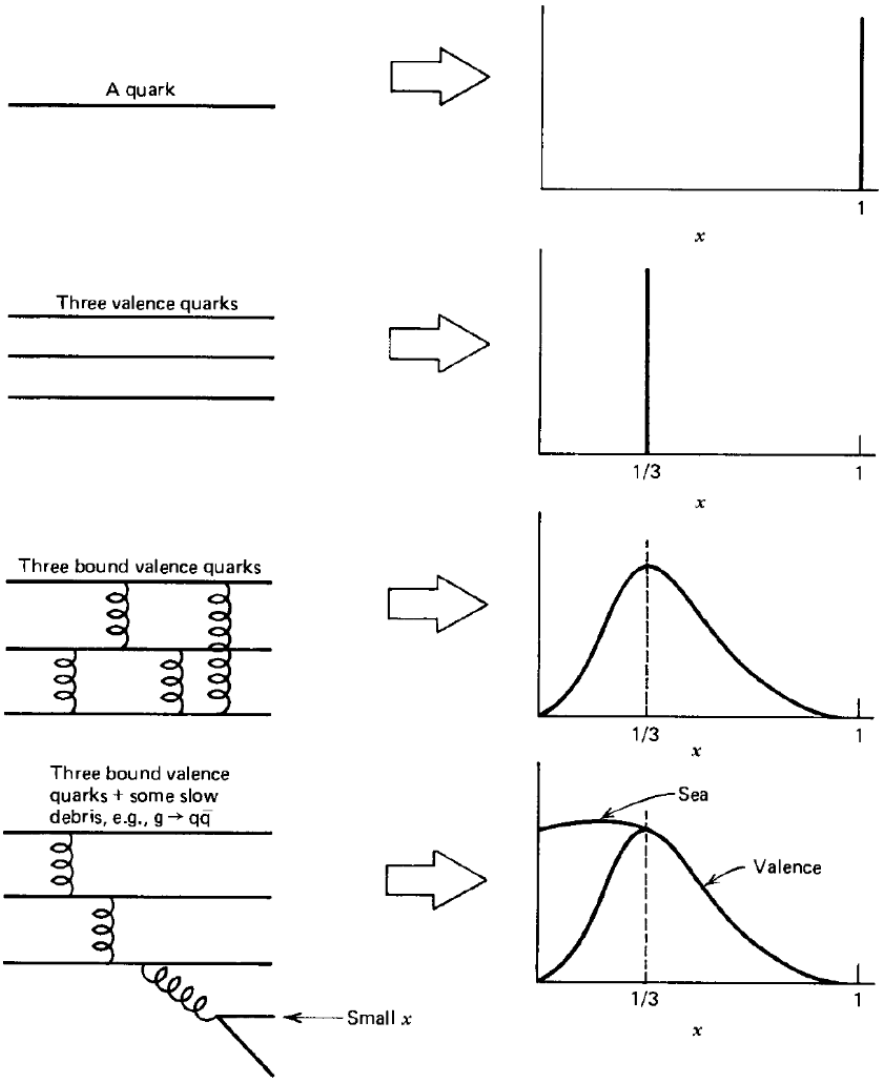

Figure 3.8: Qualitative shape of F_2 depending on the model of the proton structure. Figure from [20]

If the proton is composed of the three valence quarks, then naturally each quark is associated to a delta function and $F_2 = 3\delta\left(x_{Bj} - 1/3\right)$. If one adds interaction to the previous model, then the distributions become continuous and spread them between 0 and 1, with a peak at $1/3$. Finally, if one also considers the splitting of gluons by Bremsstrahlung into sea quark-anti quark, splitting with a probability of $\mathrm{d}x/x$, then in the small- x region, F_2 becomes non-vanishing.

We can be more quantitative. One can separate the contribution from the valence quark and the sea

quark for the up and down quarks :

$$u = u_v + m$$
$$d = d_v + m$$

with $u_m = \bar{u}_m = d_m = \bar{d}_m = s = \bar{s} = m$ if assuming the $SU(3)$ flavour symmetry [2]. Then, the proton and neutron structure functions have the form :

$$\begin{aligned} \frac{F_2^{(p)}(x_{Bj})}{x_{Bj}} &= \frac{1}{9}(4u_v + d_v) + \frac{4}{3}m \\ \frac{F_2^{(n)}(x_{Bj})}{x_{Bj}} &= \frac{1}{9}(4d_v + u_v) + \frac{4}{3}m \end{aligned} \tag{3.108}$$

Their difference gives

$$\frac{1}{x_{Bj}}\left(F_2^{(p)} - F_2^{(n)}\right) = \frac{1}{3}(u_v - d_v) \tag{3.109}$$

Experiments confirm that the difference has indeed the predictive shape in 3.8, shape when one excludes the contribution of sea quarks and gluons.

Let's analyse now the ratio $F_2^{(p)}/F_2^{(n)}$, which has the expression

$$\frac{F_2^{(p)}}{F_2^{(n)}} = \frac{4u_v + d_v + 12m}{4d_v + u_v + 12m}. \tag{3.110}$$

When $x_{Bj} \to 0$, the sea quarks and gluons outweigh the valence quark. Therefore, one expects

$$\frac{F_2^{(p)}}{F_2^{(n)}} \underset{x_{Bj}\to 0}{\to} 1 \tag{3.111}$$

In the opposite case of large momentum fraction, valence quarks should predominate, leading to:

$$\frac{F_2^{(p)}}{F_2^{(n)}} \underset{x_{Bj}\to 1}{\to} \frac{u_v + 4d_v}{4u_v + d_v} \tag{3.112}$$

From experiments, it has been found that the ratio tends to $1/4$ when x_{Bj} is large, which is in accordance with the idea that the up-quark predominates the down quark in the proton. Thus, the assumption $u_v \sim 2d_v$ is wrong as this would leads to $F_2^{(p)}/F_2^{(n)} \to 3/2$.

It has been shown that the predominant valence quark should have the form

$$f_v(x_{Bj}) \sim (1 - x_{Bj})^3$$

This is the Drell-Yan relation [14].

The power of 3 comes from the relation between the behaviour of PDFs near 1 to the asymptotic behavior of differential cross-section of deep elastic scattering. Deep elastic scattering occurs when the struck parton has a momentum fraction near one and the other constituents are sea partons. Therefore, the scattering amplitude of deep elastic scattering (and so the form factors) is proportional to the probability of having one parton with momentum fraction between 1-y and 1, with y small $\int_{1-y}^{1} \mathrm{d}x\, f i_v(x)$. One can show that this probability is of the form y^α, giving $f_v(x)(1-x)^{\alpha-1}$. One then expect $\alpha \simeq 4$ as the deep elastic cross-section is governed by $G_M \sim 1/Q^4$.

[2] From New Muon Collaboration deep inelastic muon scattering data, it was found that $\bar{d}$ is higher than $\bar{u}$ for x small

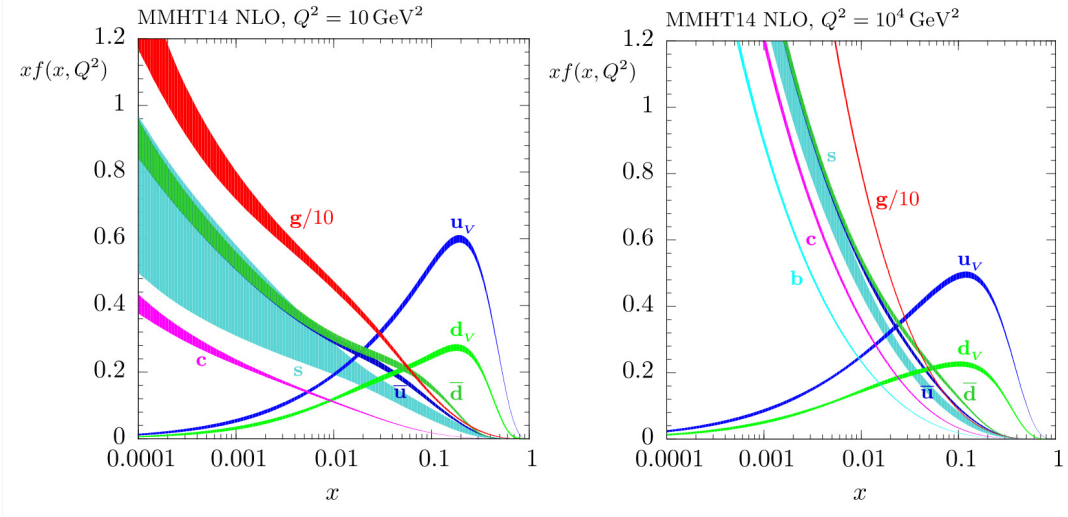

Figure 3.9: NLO PDFs at $Q^2 = 10GeV^2$ and $Q^2 = 104GeV^2$, with associated 68% confidence-level uncertainty band, using the MMHT2014 parametrisation [25]

Figure 3.9 gives the partons distributions functions from electron-proton deep inelastic scattering and other related hard scattering processes. From this figure and figure 3.10, one can see PDFs do depend on Q^2. This is especially the case in the small-x region. The resolution is going as $1/Q$ so when Q^2 increases, we can see more partons inside the nucleon. Moreover, when x is small, the sea quarks and gluons dominate in the nucleon and this dominance increases even more with the increase of Q^2. The evolution of PDFs in term of Q^2 are given by the Dokshizer Gribov Lipatov Altarelli Parisi (DGLAP) equations. Perturbative QCD can then be applied to find PDFs to different orders of the strong coupling constant α_S.

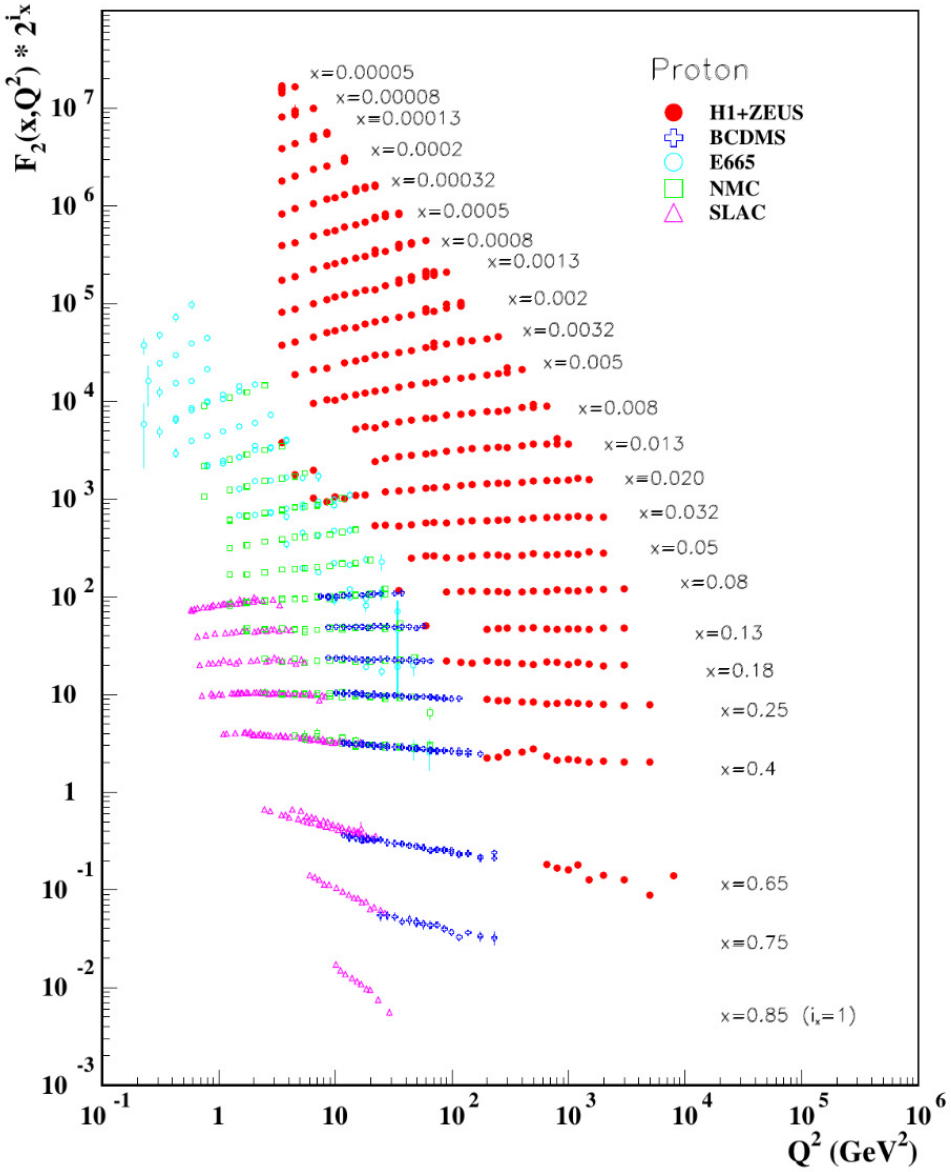

Figure 3.10: Measure of $F_2^{(p)}$ from various experiments. They are offset from each other by $2^i x$, where i is the number of x bin in descending order.

3.8 The improved parton model

Radiative corrections to the sub process $\gamma^* - parton$ are added to the naive parton model discussed in the previous section. the leading order correction $O(\alpha_s)$ correspond to the emissions of collinear gluons by either the incoming or outgoing quark. However, multiple splittings are possible and the intermediate particles in the parton cascade are increasingly virtual, meaning $x_{i+1} << x_i$. The IR divergence, from corrections and which are of the form $\left(\alpha_S(Q^2)\ln\left(Q^2/Q_0^2\right)\right)^n, n \in \mathbb{N}$ where Q_0^2 is a suitable renormalisation point are resummed. In the following, we will note by $t = \ln\left(Q^2/Q_0^2\right)$. The resummation corresponds to renormalisation group equations of the quark of flavour f:

$$\begin{aligned}\frac{\mathrm{d}q^f}{dt}(x,t) &= \frac{\alpha_S(t)}{2\pi}\int_x^1 \frac{\mathrm{d}y}{y}\left\{\sum_j q^j(y,t)(y,t)P_{qq}(\frac{x}{y} + G(y,t)P_{qG}(\frac{x}{y})\right\} \\ &= \frac{\alpha_S(t)}{2\pi}\sum_j (q^j \otimes P_{qq})(x,t) + (G \otimes P_{qG})(x,t)\end{aligned} \tag{3.113}$$

and for the gluons distributions functions:

$$\begin{aligned}\frac{\mathrm{d}G}{dt}(x,t) &= \frac{\alpha_S(t)}{2\pi}\int_x^1 \frac{\mathrm{d}y}{y}\left\{\sum_j q^j(y,t)(y,t)P_{Gq}(\frac{x}{y} + G(y,t)P_{GG}(\frac{x}{y})\right\} \\ &= \frac{\alpha_S(t)}{2\pi}\sum_j (q^j \otimes P_{Gq})(x,t) + (G \otimes P_{GG})(x,t)\end{aligned} \tag{3.114}$$

The P functions are called the splitting functions.

It is easier to understand the meaning of these equations if one considers having only one flavour and if one defines $q'_{NS}(x,t) = q(x,t) - \bar{q}(x,t)$, the "net" number of quarks in the proton from the point of γ^*. $q_{NS}(x,t)$ DGLAP equation can rewritten as

$$q_{NS}(x,t) + \mathrm{d}q_{NS}(x,t) = \int_0^1 \mathrm{d}y \int_0^1 \mathrm{d}z \quad \delta(zy-x)q_{NS}(y,t)\left[\delta(z-1) + \frac{\alpha(t)}{2\pi}P_{qq}(z)\mathrm{d}t\right] \tag{3.115}$$

From (3.115), we can see that the number of net quarks with fraction momentum x changes with the infinitessimal variation of resolution dt. Starting from a quark with fraction momentum y, it can either already have momentum $x = y$ and not radiate or it can split into a collinear gluon and a quark of fraction momentum $x = zy$. $Pqq(z)$ is then, for $z < 1$, the probability density of finding a quark inside the parent quark with fraction z of the parent momentum.

The splitting functions have the following properties.

The conservation quarks, anti quarks leads to

$$\int_0^1 \mathrm{d}z\, P_{qq}(z) = 0 \tag{3.116}$$

The conservation of proton total momentum $\frac{\mathrm{d}}{\mathrm{d}t}\int_0^1 \mathrm{d}x x\left[\sum_{i=1}^L q^i(x,t) + G(x,t)\right] = 0$ results in:

$$\int_0^1 \mathrm{d}z \quad z\left[P_{\mathrm{qq}}(z) + P_{\mathrm{Gq}}(z)\right] = 0 \tag{3.117}$$

$$\int_0^1 \mathrm{d}z \quad z\left[n_f P_{\mathrm{qG}}(z) + P_{\mathrm{GG}}(z)\right] = 0 \tag{3.118}$$

Their expression are found using quark, anti quark and gluon splitting vertices, as explained in [1] :

$$P_{qq}(z) = C_F\left(\frac{1+z^2}{1-z}\bigg|_+ + \frac{3}{2}\delta(1-z)\right) \tag{3.119}$$

$$P_{qG}(z) = \frac{1}{2}\left(z^2 + (1-z)^2\right) \tag{3.120}$$

$$P_{Gq}(z) = C_F\frac{1+(1-z)^2}{z} \tag{3.121}$$

$$P_{GG}(z) = 2C_A\left(\frac{z}{(1-z)}\bigg|_+ + \frac{1-z}{z} + z(1-z)\right) + \left(\frac{11}{6}C_A - \frac{1}{3}n_f\right)\delta(1-z) \tag{3.122}$$

where

$$\int_0^1 \frac{f(x)}{(1-x)_+}dx = \int_0^1 \frac{f(x)-f(1)}{1-x}dx. \tag{3.123}$$

is the "+" prescription which regularize $1/(1-z)$, when associated with the term proportional to $\delta(1-z)$, at the singularity $z = 1$. This corresponds to taking into account virtual corrections (self-energy and virtual exchange of gluons). which cancel the emissions of soft gluons, that leads to these soft IR divergences.

Chapter 4

Conclusion

In this dissertation, we saw how QCD is a good theory of the strong interaction, especially because of its non-abelian nature leading to asymptotic freedom. One important concept of this theory is the parton model, which is used, with perturbative QCD, to analyse and predict experimental results for hadronic processes. As seen, form factors and PDFs, which are subject to integro-differential equations similar to renormalisation group equations, are two key ways to characterize the structure of the nucleons and their measures can be done through lepton-nucleon scattering. Many aspects have not been covered in this dissertation. The first one is all the other ways that the inner structure of the nucleon can be characterized. One of them is the Transverse Momentum Distribution, which is an extension to the idea of PDF and include the transverse momentum as a variable in the distribution. Another one is the inclusion of spin in the PDFs and the determination of how the spin of the proton is distributed among its different constituents. From a more theoretical point of view, discussions on saturation occuring the small-x limit and the theory of Color Glass Condensate habe also been omitted.

Future experiments such as those that will be realised in the new Electron-Ion Collider (EIC) or at LHeC, will increase the precision on the measures of PDFs, especially at the extreme regions of x_{Bj}, large-x and small-x, region where asymmetry for the sea quarks has been recently observed between the ani-up and anti-down quark. Those measures will then make experimental predictions on hard hadronic processes more accurate.

Appendices

Appendix A

Color factors

We note by T^a generators of a quelconque represnetation of SU(N) and by t^a the generators in the fundamental representation.

Some useful relationships to calculate color factors :

$$\begin{aligned}
\mathrm{Tr}\left(T^a\right) &= 0 \\
\left[T^a, T^b\right] &= i f^{abc} T^c,\ f^{abc} \text{ totally anti symmetric} \\
\left\{t^a, t^b\right\} &= \frac{\delta^{ab}}{N} + d^{abc} T^c,\ d^{abc} \text{ totally symmetric} \\
\sum_{cd} d^{acd} d^{bcd} &= \left(N - \frac{4}{N}\right) \delta^{ab} \\
\mathrm{Tr}\left(t^a t^b\right) &= \frac{1}{2}\delta^{ab} \text{ Usual normalisation} \\
t^a_{ij} t^a_{kl} &= \frac{1}{2}\left(\delta_{il}\delta_{jk} - \frac{1}{N}\delta_{ij} kl\right) \text{ Fierz identity}
\end{aligned}$$

I will now give two typical color factors.

In the fundamental representation, the color factor is :

$$(t^a t^b)_{ij} = C_F \delta_{ij} = \frac{N^2 - 1}{2N}\delta_{ij}$$

We note that $t^a t^a$ is a Casimir operator ie commutes with the generators of SU(N) so commutes with all elements of the Lie algebra. Hence, from Schur's lemma, $t^a t^a = C_F \mathbb{1}$. Tracing this relation gives the value of C_F.

The color factor in the adjoint representation is :

$$f^{acd} f^{bcd} = C_A \delta^{ab} = N \delta ab$$

It is possible to calculate color factors using a graphical methods. Examples and details can be found in [37]

Appendix B

Notes on path integral

The fundamental question that the path-integral approach of quantum mechanics answer is the calculation the transition amplitude that a particle at $q(t_0) = x_i$ will go to $q(t_f) = x_f$. In this formulation, one finds that the probability amplitude takes the form :

$$\left\langle x_f \middle| e^{-i\hat{H}(t_f - t_0)} \middle| x_i \right\rangle = \int_{x_i}^{x_f} Dq(t) \int Dp(t) \exp\left(\int_{t_0}^{t_f} \mathrm{d}t\, p\dot{q} - H(p,q) \right) \tag{B.1}$$

where q and p the position and momentum. The dimension of the phase space is 2d.

The functional integral $\int Dq(t)$ and $\int Dp(t)$ are defined by :

$$\begin{aligned} \int_{x_i}^{x_f} Dq(t) &= \lim_{N \to +\infty} \Pi_{n=0}^{N-1} \mathrm{d}^d q_i \quad q_0 = x_i \text{ and } q_N = x_f \\ \int Dp &= \lim_{N \to +\infty} \Pi_{n=0}^{N-1} \frac{\mathrm{d}^d p_i}{(2\pi)^d} \end{aligned} \tag{B.2}$$

Integrating (B.1) gives the configuration space $(q, \dot{q})$ path integral :

$$\left\langle x_f \middle| e^{-i\hat{H}(t_f - t_0)} \middle| x_i \right\rangle = \mathcal{N} \int_{x_i}^{x_f} Dq(t) e^{iS[q(t)]} \tag{B.3}$$

where S is the action dependent of $q, \dot{q}$ and $\mathcal{N}$ is a normalisation factor.

(B.3) is the generalisation of the principle of least action to quantum mechanics and can be extended to quantum field theory, where then the variables are the fields themselves.

One important concept in path-integral quantum field theory is the generating function :

$$Z[J] = \int D\phi \exp\left(iS(\phi) + i \int \mathrm{d}^d x\, J(x)\phi(x) \right) \tag{B.4}$$

which is used to calculate Green's functions through the relation

$$G_n(x_1, ..., x_n) = \langle \Omega | \hat{T} \phi(x_1) ... \phi(x_n) | \Omega \rangle = (-i)^n \frac{\delta^n}{\delta J(x_1) ... \delta J(x_n)} \left(\frac{Z[J]}{Z[0]} \right) \Bigg|_{J=0} \tag{B.5}$$

with ϕ a scalar field and $\int \mathrm{d}^d x\, J(x)\phi(x)$ is the source term.

For fermionic fields, the same kind of generating functions are defined but on should be careful as then functional integral and sources are Grassmannian.

Appendix C

β-function through the Background Field method

C.1 Background method

We will outline the calculation to derive the first-order β_V-function. This is based on the lecture notes of Andrew J. Tolley and on [33]. We neglect the mass of the fermions in those calculations.

The Background field method consists at separating the gauge fields into fixed, classical fields $A^a_\mu(x)$ plus quantum correction $W^a_\mu(x)$ ie

$$\mathcal{A}^a_\mu(x) = A^a_\mu(x) + gW^a_\mu(x) \tag{C.1}$$

g here plays the same role as $\sqrt{\hbar}$ when we separate in the same way for the fermionic fields.

The equation for the one-particle irreducible (1PI) effective action is :

$$\begin{aligned}\exp\left(i\Gamma(A,B,\psi_*,\bar{\psi_*})\right) &= \int D\mathcal{A}\int D\mathcal{B}\int D\bar{c}\int Dc\int D\psi\int D\bar{\psi}\; e^{iS_{BRST}+\int \mathrm{d}^dx\bar{\psi}(i\not{D})\psi - isource\ terms} \\ &= e^{i\Gamma(A,B)}e^{\Gamma(\psi,\bar{\psi})}\end{aligned} \tag{C.2}$$

$Peskin : 1995ev$(C.3

where $S_{BRST} = \int \mathrm{d}^dx\,(\frac{1}{4}(F^a_{\mu\nu})^2 + B^aF^a(A_\mu) + \frac{\xi}{2}B^{a2} + \int \mathrm{d}^dy\,\bar{c}^a(x)\frac{\delta F^a(A_\mu)(x)}{\delta\theta^b(y)}c^b(y))$ and the source terms are $\int \mathrm{d}^dx\left(J^a_\mu(\mathcal{A}^a_\mu - A^a_\mu) + K^a(\mathcal{B}^a - B^a) + (\bar{\psi}-\bar{\psi}_*)\eta + \bar{\eta}(\psi-\psi_*)\right)$
$J, K, \eta, \bar{\eta}$ are such that :

$$\begin{aligned}-J^a_\mu(x) &= \frac{\delta\Gamma}{\delta A^a_\mu(x)} \\ -K^a(x) &= \frac{\delta\Gamma}{\delta B^a(x)} \\ -\eta^a &= \frac{\delta\Gamma}{\delta\bar{\psi_*}(x)} \\ -\bar{\eta^a} &= \frac{\delta\Gamma}{\delta\psi_*(x)}\end{aligned}$$

We rescale the fields :

$$\mathcal{A}_\mu \to \frac{1}{g}\mathcal{A}_\mu$$
$$\mathcal{B} \to \frac{1}{g}\mathcal{B}$$
$$A \to \frac{1}{g}A$$

From this rescaling, we then have :

$$F^2_{\mu\nu} \to \frac{1}{g^2}F^2_{\mu\nu}$$
$$D_\mu \to \partial_\mu - iA^a_\mu t^a$$

Moreover, from (C.1), we have :

$$\mathcal{F}^a_{\mu\nu} = F^a_{\mu\nu} + gD_{\overset{a}{\nu} - gD_\nu W^a_\mu + g^2 f^{abc} W^b_\mu W^c_\nu}$$
$$\mathcal{D}_\mu = D_\mu - igW^a_\mu$$

The gauge is fixed to : $F^a(A_\mu) = D^\mu(\mathcal{A}^a_\mu - A^a_\mu)$ with D_μ the covariant gauge w.r.t A^a_μ. From the infinitessimal form of the gauge transformation $\delta A^a_\mu = (D_\mu\theta)^a$, we have $\frac{\delta F^a(A_\mu)(x)}{\delta\theta^b(y)} = (D^\mu\mathcal{D}_\mu)^{ab}\delta^{(d)}(x-y)$

By choosing B such that $\frac{\delta\Gamma}{\delta B} = 0$ and integrating w.r.t B, the new gauge fixed Lagrangian is :

$$\begin{aligned}\mathcal{L} \quad &= -\tfrac{1}{4g^2}(F^a_{\mu\nu})^2 - \tfrac{1}{g}F^{\mu\nu a}(D_\mu W_\nu)^a - \tfrac{1}{2}F^{\mu\nu a}f^{abc}W^b_\mu W^c_\nu - \tfrac{1}{4}(D_\mu W^a_\nu - D_\nu W^a_\mu)^2 \\ &-\tfrac{1}{2\xi}(D^\mu W^a_\mu)^2 + \bar{c^a}(-(D^2)^{ac} - f^{abc}(D^\mu W_\mu)^b)c^c + \bar{\psi}(i\not{D} + gW^a_\mu\gamma^\mu t^a)\psi\end{aligned} \tag{C.4}$$

This Lagrangian is invariant under the local background gauge symmetry $\delta A^a_\mu = D_\mu\theta^a$ under which $W_\mu, c, \bar{c}$ transform as :

$$W^a_\mu \to W^a_\mu - f^{abc}\theta^b A^c_\mu$$
$$\psi \to \psi + i\theta^a t^a\psi$$
$$c^a \to -f^{abc}\theta^b c^c$$

C.2 One-loop effective action

In those calculation of the expression of the one loop effective action, I drop linear terms in W_μ as they aren't of interest here.

C.2.1 Fermions one loop effective action

We redefine the fermionic fields :

$$\psi = \psi_* + \chi\sqrt{\hbar}$$
$$\bar{\psi} = \bar{\psi}_* + \bar{\chi}\sqrt{\hbar}$$

The calculation only goes to the one-loop effective action ie order $\sqrt{\hbar}$. Hence, in the source terms with $\frac{\delta\Gamma}{\delta\psi_*}$ and $\frac{\delta\Gamma}{\delta\bar{\psi}_*}$, the partial derivatives only need to be calculated to the zero-order as the terms into bracket already is of order $\sqrt{\hbar}$.

Hence, the one loop effective action is defined by :

$$\begin{aligned} e^{i\Gamma_{\text{one-loop}}} &= \int D\chi \int D\bar{\chi}\ \exp\{i \int \mathrm{d}^d x\, \bar{\chi}(i\not{D})\chi\} \\ &= (\det(i\not{D}))^{n_f} \end{aligned} \tag{C.5}$$

with n_f the number of flavour of fermions

The square root of the covariant derivative operator is used instead of directly calculating $\det(i\not{D})$:

$$\begin{aligned} \Delta = (i\not{D})^2 &= -\gamma^\mu\gamma^\nu D_\mu D_\nu \\ &= -\tfrac{1}{2}\{\gamma^\mu,\gamma^\nu\} D_\mu D_\nu - \tfrac{1}{2}[\gamma^\mu,\gamma^\nu] D_\mu D_\nu \\ &= -D^2 + 2iS^{\mu\nu}[D_\mu D_\nu] \text{ par anti-symmetry of } S^{\mu\nu} = \tfrac{i}{4}[\gamma^\mu,\gamma^\nu]] \\ &= -D^2 + F^b_{\mu\nu} S^{\mu\nu} t^b \end{aligned} \tag{C.6}$$

Hence, the fermions give a contribution of

$$\Gamma_{\text{one-loop}} = -i\frac{n_f}{2}\operatorname{Tr}(\ln\Delta) \tag{C.7}$$

They give no contribution to the β_V- function so I will from now on ignore this part.

C.2.2 Gauge and ghost field one loop effective action

Using (C.4) and the same argument as in C.2.1, the one loop effective action for the gauge field is defined by the equation:

$$\begin{aligned} e^{i\Gamma_{\text{one-loop}}(A)} &= \int DW \int Dc \int D\bar{c}\ \exp\{i \int \mathrm{d}^d x\, (\tfrac{1}{2} W^a_\mu \hat{O}^{ab\mu\nu} W^b_\nu - \bar{c}^a (D_\mu D^\mu)^{ab} c^b)\} \\ &= \frac{1}{\sqrt{\det(\hat{O}^{ab}_{\mu\nu})}} \det\big((D_\mu D^\mu)^{ab}\big) \end{aligned} \tag{C.8}$$

where

$$\int \mathrm{d}^{dd} x\, \frac{1}{2} W^{\mu a} \hat{O}^{ab}_{\mu\nu} W^{\nu b} = \int \mathrm{d}^d x \left(-\frac{1}{2}(D_\mu W^a_\nu)^2 + \frac{1}{2}(D_\mu W_\nu)^a (D^\nu W^\mu)^a - \frac{1}{2\xi}(D^\mu W^a_\mu)^2 - \frac{1}{2} F^{\mu\nu a} f^{abc} W^b_\mu W^c_\nu \right) \tag{C.9}$$

Therefore, the one loop effective action for the gauge field is

$$\Gamma_{\text{one-loop}} = \frac{i}{2}\operatorname{Tr}\left(\ln \hat{O}^{ab}_{\mu\nu}\right) - i\operatorname{Tr}\left(\ln (D_\mu D^\mu)^{ab}\right) \tag{C.10}$$

C.3 Computations of the β_V function

We will note $\hat{P}^{ab} = (D_\mu D^\mu)^{ab}$ and ignore in this part the fermions contribution to the running of the strong coupling constant. To simplify the calculations, we choose to perform them with the Feynman gauge meaning $\xi = 1$. (C.9) then becomes,

$$\begin{aligned} \hat{O}^{ab}_{\mu\nu} &= (D^\omega D_\omega)^{ab} g_{\mu\nu} + (D_\mu D_\nu)^{ab} - (D_\nu D_\mu)^{ab} - F_\mu \nu^c f^{cab} \\ &= (D^\omega D_\omega)^{ab} g_{\mu\nu} - 2F^c_{\mu\nu} f^{cab} \end{aligned} \tag{C.11}$$

as $[D_\mu, D_\nu]^{ab} = -F^c_{\mu\nu} f^{cab}$ in the adjoint representation.

To lowest order, it is only necessary to find corrections coming from quadratic terms. To do that, one technique is to vary twice $\Gamma_{\text{one-loop}}$ and then set $A = 0$.

Varying twice the 1PI effective action gives

$$\delta^2 \Gamma_{\text{oneloop}} = \frac{i}{2} \operatorname{Tr}\left(\frac{1}{\hat{O}} \delta^2 \hat{O}\right) - \frac{i}{2} \operatorname{Tr}\left(\frac{1}{\hat{O}} \delta\hat{O} \frac{1}{\hat{O}} \delta\hat{O}\right) - i \operatorname{Tr}\left(\frac{1}{\hat{P}} \delta^2 \hat{P}\right) + i \operatorname{Tr}\left(\frac{1}{\hat{P}} \delta\hat{P} \frac{1}{\hat{P}} \delta\hat{P}\right) \tag{C.12}$$

Varying A of δA leads to :

$$\begin{aligned} \delta F^c_{\mu\nu} &= D_\mu \delta A^c_\nu - D_\nu \delta A^c_\mu \\ (\delta(D_\mu)\phi)^a &= f^{abc} \delta A^b_\mu \phi^c = -i(T^b)_{ac} \delta A^b_\mu \phi^c \end{aligned}$$

with ϕ a field in the adjoint representation.

After varying $\hat{O}$ and $\hat{P}$ and then setting $A = 0$, the different elements in (C.12) have the expressions below :

$$\begin{aligned} \hat{O}^{ab}_{\mu\nu} &= \Box \delta^{ab} g_{\mu\nu} \\ \delta\hat{O}^{ab}_{\mu\nu} &= -iT^c_{ab} \hat{Y}^c g_{\mu\nu} - 2iB^c_{\mu\nu} T^c_{ab} \\ \delta^2 \hat{O}^{ab}_{\mu\nu} &= -\left(T^d T^e + T^e T^d\right)^{ab} \delta A^d_\omega \delta A^e_\omega g_{\mu\nu} + 2iT^d_{ce} \left(\delta A^d_\mu \delta A^e_\nu - \delta A^d_\nu \delta A^e_\mu\right) f^{cab} \\ \hat{P}^{ab} &= \Box \delta^{ab} \\ \delta\hat{P}^{ab} &= -iT^c_{ab} \hat{Y}^c \\ \delta^2 \hat{P}^{ab} &= -2(T^c T^d)_{ab} \delta A^c_\mu a^c_\mu \end{aligned} \tag{C.13}$$

where $\hat{Y} = (\delta A^c_\omega \partial^\omega + \partial_\omega \delta A^{c\omega})$ and $B^c_{\mu\nu} = \left(\partial_\mu \delta A^c_\nu - \partial_\nu A^c_\mu\right)$

Using (C.13) and evaluating the trace over the gauge group and over the metric, (C.12) becomes :

$$\begin{aligned} \delta^2 \Gamma_{\text{one-loop}} &= -i(d-2) C_A \operatorname{Tr}_s\left(\tfrac{1}{\Box} \delta A^d_\mu A^{\mu d}\right) + \tfrac{i}{2} C_A (d-2) \operatorname{Tr}_s\left(\tfrac{1}{\Box} \hat{Y}^c \tfrac{1}{\Box} \hat{Y}^c\right) \\ &\quad -2iC_A \operatorname{Tr}_s\left(\tfrac{1}{\Box} B^c_{\mu\nu} \tfrac{1}{\Box} B^c_{\mu\nu}\right) \end{aligned} \tag{C.14}$$

with C_A the quadratic Casimir operator in the adjoint representation and Tr_s the trace over just the operators.

In order to evaluate the different traces in (C.14), the operators need to be expressed in momentum space:

$$\begin{aligned} \langle p | \tfrac{1}{\Box} | p' \rangle &= -\tfrac{1}{p^2} (2\pi)^d \delta^{(d)}(p - p') \\ \langle p | \delta A^{c\omega} | p' \rangle &= \delta \tilde{A}^{c\omega}(p - p') \\ \langle p | B^c_{\mu\nu} | p' \rangle &= \tilde{B}^c_{\mu\nu}(p - p') \\ \langle p | \hat{Y}^c | p' \rangle &= i(p' + p)_\omega \delta \tilde{A}^{c\omega}(p - p') \end{aligned} \tag{C.15}$$

The first two terms in (C.14) give then a contribution of

$$F_1 = \int \frac{\mathrm{d}^d k}{(2\pi)^d} \delta\tilde{A}^{c\mu}(-k)\delta\tilde{A}^{c\nu}(k)F_{\mu\nu}(k) \tag{C.16}$$

with

$$F_{\mu\nu}(k) = -\frac{i}{2}C_A(d-2)\int \frac{\mathrm{d}^d p}{(2\pi)^d}\frac{1}{p^2(p+k)^2}\left[(2p_\mu + k_\mu)(2p_\nu + k_\nu) - 2g_{\mu\nu}(p+k)^2\right] \tag{C.17}$$

Using Feynman parametrisation, Wick rotation, doing a dimensional regularisation with $d = 4-\epsilon$ and using the Legendre duplication formula for the Gamma function $\Gamma(z)\Gamma(z+\frac{1}{2}) = 2^{1-2z}\sqrt{\pi}\Gamma(2z)$, the previous expression becomes :

$$F_{\mu\nu}(k) = (d-2)2C_A 2^{-2d}\pi^{\frac{1}{2}-\frac{d}{2}}\frac{\Gamma(\frac{d}{2}-1)\Gamma(2-\frac{d}{2})}{\Gamma(\frac{d+1}{2})}(k^2)^{\frac{d-4}{2}}(k_\mu k_\nu - k^2 g_{\mu\nu}) \tag{C.18}$$

The last term give a contribution of

$$F_2 = \int \frac{\mathrm{d}^d k}{(2\pi)^d} \delta\tilde{A}^{c\mu}(-k)\delta\tilde{A}^{c\nu}(k)G_{\mu\nu}(k) \tag{C.19}$$

with

$$G_{\mu\nu}(k) = 2i\int \frac{\mathrm{d}^d p}{(2\pi)^d} 2C_A \frac{1}{p^2(p+k)^2}(k_\mu k_\nu - g_{\mu\nu}k^2) \tag{C.20}$$

Through the same process, $G_{\mu\nu}$ becomes :

$$G_{\mu\nu} = -2C_A 2^{4-2d}\pi^{\frac{1}{2}-\frac{d}{2}}\frac{\Gamma(2-\frac{d}{2})\Gamma(\frac{d}{2}-1)}{\Gamma(\frac{d-1}{2})}(k^2)^{\frac{d-4}{2}}(k_\mu k_\nu - g_{\mu\nu}k^2) \tag{C.21}$$

The sum of $G_{\mu\nu}(k)$ and $F_{\mu\nu}(k)$ gives :

$$\begin{aligned} F_{\mu\nu} + G_{\mu\nu} &= (k_\mu k_\nu - g_{\mu\nu}k^2)(k^2)^{-\frac{\epsilon}{2}}\left[2C_A 2^{-2d}\pi^{\frac{1}{2}-\frac{d}{2}}\Gamma(\frac{d}{2}-1)\Gamma(2-\frac{d}{2})\left(\frac{d-2}{\Gamma(\frac{d+1}{2})} - \frac{2^4}{\Gamma(\frac{d-1}{2})}\right)\right] \\ &= (k_\mu k_\nu - g_{\mu\nu}k^2)(k^2)^{-\frac{\epsilon}{2}}c_d \end{aligned}$$

$\delta^2\Gamma_{\text{one-loop}}$ corrects the tree-level 1PI effective action

$$\Gamma_{\text{tree}} = \int \mathrm{d}^d x\, \mu^{-\epsilon} - \frac{1}{4g^2}F^e_{\mu\nu}F^{\mu\nu e}$$

The arbitrary parameter μ here is to keep the coupling constant g dimensionless.

Deriving this twice and only keeping to quadratic order in the fields gives

$$\delta^2\Gamma_{\text{tree}} = \mu^{-\epsilon}\int \frac{\mathrm{d}^d k}{(2\pi)^d}\frac{1}{g^2}\delta\tilde{A}^{\mu c}(-k)\delta\tilde{A}^{\nu c}(k)(k_\mu k_\nu - k^2 g_{\mu\nu}) \tag{C.22}$$

Adding (C.14) to (C.22) gives then :

$$\delta^2\Gamma = \mu^{-\epsilon}\int \frac{\mathrm{d}^d k}{(2\pi)^d}\frac{1}{g^2_{phy}}\delta\tilde{A}^{\mu c}(-k)\delta\tilde{A}^{\nu c}(k)(k_\mu k_\nu - k^2 g_{\mu\nu}) \tag{C.23}$$

with

$$\frac{1}{g^2_{phy}} = \frac{1}{g^2} + c_d\left(\frac{\mu}{k}\right)^\epsilon \tag{C.24}$$

g_{phy} is the physical coupling constant. hence, it should be independent of the arbitrary parameter μ. This constraint leads to the renormalisation group equation for the coupling constant.

More concretely, the constraint is :

$$\frac{\mathrm{d}}{\mathrm{d}\ln\left(\frac{\mu}{k}\right)}\left(\frac{1}{g_{phy}^2}\right) = 0$$

giving then

$$\frac{\mathrm{d}g}{\mathrm{d}\ln\left(\frac{\mu}{k}\right)} = \frac{1}{2}d_0 g^3 \tag{C.25}$$

with the constant $d_0 = \lim_{\epsilon\to 0} \epsilon c_d$

More precisely,using $\Gamma(1-z)\Gamma(z) = \frac{\pi}{\sin(\pi z)}, \quad z \notin \mathbb{Z}$ and some specific values of the Gamma function $\Gamma(\frac{5}{2}) = \frac{3}{4}\sqrt{\pi}$ and $\Gamma(\frac{3}{2}) = \frac{\sqrt{\pi}}{2}$

$$d_0 = 2C_A \frac{1}{(4\pi^2)}\left(-\frac{11}{3}\right)$$

Hence,

$$\beta_V \equiv \frac{\mathrm{d}g}{\mathrm{d}\ln\left(\frac{\mu}{k}\right)} = C_A \frac{g^3}{(4\pi)^2}\left(-\frac{11}{3}\right) \tag{C.26}$$

Bibliography

[1] Guido Altarelli and G. Parisi. Asymptotic Freedom in Parton Language. *Nucl. Phys. B*, 126:298–318, 1977.

[2] L. Andivahis, P. E. Bosted, A. Lung, L. M. Stuart, J. Alster, R. G. Arnold, C. C. Chang, F. S. Dietrich, W. Dodge, R. Gearhart, J. Gomez, K. A. Griffioen, R. S. Hicks, C. E. Hyde-Wright, C. Keppel, S. E. Kuhn, J. Lichtenstadt, R. A. Miskimen, G. A. Peterson, G. G. Petratos, S. E. Rock, S. Rokni, W. K. Sakumoto, M. Spengos, K. Swartz, Z. Szalata, and L. H. Tao. Measurements of the electric and magnetic form factors of the proton from q^2=1.75 to 8.83 (gev/c)^2. *Phys. Rev. D*, 50:5491–5517, Nov 1994.

[3] P.A. Baikov, K.G. Chetyrkin, and J.H. Kühn. Five-loop running of the qcd coupling constant. *Physical Review Letters*, 118(8), Feb 2017.

[4] W. Bartel, F.-W. Büsser, W.-R. Dix, R. Felst, D. Harms, H. Krehbiel, P.E. Kuhlmann, J. McElroy, J. Meyer, and G. Weber. Measurement of proton and neutron electromagnetic form factors at squared four-momentum transfers up to 3 (gev/c)2. *Nuclear Physics B*, 58(2):429 – 475, 1973.

[5] A. V. Belitsky, Xiangdong Ji, and Feng Yuan. Perturbative qcd analysis of the nucleon's pauli form factorf2(q2). *Physical Review Letters*, 91(9), 2003.

[6] Ch. Berger, V. Burkert, G. Knop, B. Langenbeck, and K. Rith. Electromagnetic form factors of the proton at squared four-momentum transfers between 10 and 50 fm2. *Physics Letters B*, 35(1):87 – 89, 1971.

[7] J. D. Bjorken. Asymptotic sum rules at infinite momentum. *Physical Review*, 179(5):1547–1553, 1969.

[8] J.D. Bjorken and Emmanuel A. Paschos. Inelastic Electron Proton and gamma Proton Scattering, and the Structure of the Nucleon. *Phys. Rev.*, 185:1975–1982, 1969.

[9] F. Borkowski, G. G. Simon, V. H. Walther, and R. D. Wendling. On the determination of the proton rms-radius from electron scattering data. *Zeitschrift für Physik A Atoms and Nuclei*, 275(1):29–31, 1975.

[10] P. E. Bosted, L. Andivahis, A. Lung, L. M. Stuart, J. Alster, R. G. Arnold, C. C. Chang, F. S. Dietrich, W. Dodge, R. Gearhart, J. Gomez, K. A. Griffioen, R. S. Hicks, C. E. Hyde-Wright, C. Keppel, S. E. Kuhn, J. Lichtenstadt, R. A. Miskimen, G. A. Peterson, G. G. Petratos, S. E. Rock, S. Rokni, W. K. Sakumoto, M. Spengos, K. Swartz, Z. Szalata, and L. H. Tao. Measurements of the electric and magnetic form factors of the proton from q^2=1.75 to 8.83 (gev/c)^2. *Phys. Rev. Lett.*, 68:3841–3844, Jun 1992.

[11] Stanley J. Brodsky and Glennys R. Farrar. Scaling laws for large-momentum-transfer processes. *Physical review D : Particles and fields*, 11(5):1309–1330, 1975.

[12] M. E. Christy, A. Ahmidouch, C. S. Armstrong, J. Arrington, R. Asaturyan, S. Avery, O. K. Baker, D. H. Beck, H. P. Blok, C. W. Bochna, and et al. Measurements of electron-proton elastic cross sections for0.4<q2<5.5(gevc)2. *Physical Review C*, 70(1), Jul 2004.

[13] D.H. Coward et al. ELECTRON - PROTON ELASTIC SCATTERING AT HIGH MOMENTUM TRANSFERS. *Phys. Rev. Lett.*, 20:292–295, 1968.

[14] S.D. Drell and Tung-Mow Yan. Connection of Elastic Electromagnetic Nucleon Form-Factors at Large Q**2 and Deep Inelastic Structure Functions Near Threshold. *Phys. Rev. Lett.*, 24:181–185, 1970.

[15] Sidney D Drell and Tung-Mow Yan. Partons and their applications at high energies. *Annals of Physics*, 66(2):578 – 623, 1971.

[16] Richard P. Feynman. Very high-energy collisions of hadrons. *Phys. Rev. Lett.*, 23:1415–1417, 1969.

[17] R.P. Feynman. Photon-hadron interactions. 1973.

[18] J. R. Forshaw and D. A. Ross. *Quantum Chromodynamics and the Pomeron*. Cambridge Lecture Notes in Physics. Cambridge University Press, 1997.

[19] David J. Gross and Frank Wilczek. Ultraviolet behavior of non-abelian gauge theories. *Phys. Rev. Lett.*, 30:1343–1346, Jun 1973.

[20] Francis Halzen and Alan Martin. *Quarks & Leptons: An introductory course in modern particle physics*. John Wiley & Sons, New York, USA, 1984.

[21] L. N. Hand, D. G. Miller, and Richard Wilson. Electric and magnetic form factors of the nucleon. *Rev. Mod. Phys.*, 35:335–349, Apr 1963.

[22] L. N. Hand, D. G. Miller, and Richard Wilson. Electric and magnetic form factors of the nucleon. *Reviews of Modern Physics*, 35(2):335–349, 1963.

[23] G. Hanson, M. S. Alam, A. M. Boyarski, M. Breidenbach, F. Bulos, J. T. Dakin, J. M. Dorfan, G. J. Feldman, G. E. Fischer, D. Fryberger, and et al. Hadron production by e^+e annihilation at center-of-mass energies between 2.6 and 7.8 gev. ii. jet structure and related inclusive distributions. *Physical review D : Particles and fields*, 26(5):991–1012, 1982.

[24] K. M. Hanson, J. R. Dunning, M. Goitein, T. Kirk, L. E. Price, and Richard Wilson. Large-angle quasielastic electron-deuteron scattering. *Phys. Rev. D*, 8:753–778, Aug 1973.

[25] L. A. Harland-Lang, A. D. Martin, P. Motylinski, and R. S. Thorne. Parton distributions in the lhc era: Mmht 2014 pdfs. *The European Physical Journal C*, 75(5), May 2015.

[26] T. Janssens, R. Hofstadter, E. B. Hughes, and M. R. Yearian. Proton form factors from elastic electron-proton scattering. *Phys. Rev.*, 142:922–931, Feb 1966.

[27] J. Litt, G. Buschhorn, D.H. Coward, H. Destaebler, L.W. Mo, R.E. Taylor, B.C. Barish, S.C. Loken, J. Pine, J.I. Friedman, G.C. Hartmann, and H.W. Kendall. Measurement of the ratio of the proton form

factors, ge/gm, at high momentum transfers and the question of scaling. *Physics Letters B*, 31(1):40 – 44, 1970.

[28] G. Miller, E. D. Bloom, G. Buschhorn, D. H. Coward, H. Destaebler, J. Drees, C. L. Jordan, L. W. Mo, R. E. Taylor, J. I. Friedman, and et al. Inelastic electron-proton scattering at large momentum transfers and the inelastic structure functions of the proton. *Physical review D : Particles and fields*, 5(3):528–544, 1972.

[29] N.K. Nielsen. Asymptotic freedom as a spin effect. *Am. J. Phys.*, 49:1171, 1981.

[30] C.F. Perdrisat, V. Punjabi, and M. Vanderhaeghen. Nucleon electromagnetic form factors. *Progress in Particle and Nuclear Physics*, 59(2):694–764, Oct 2007.

[31] Charles Perdrisat. *The recoil polarization experiments at Jefferson Lab.* 2014.

[32] D.H. Perkins. Neutrino interactions. In *Proc. of the 16th Int. Conf. on High Energy Physics*, volume 4, pages 189–248, Batavia, 1972.

[33] Michael E. Peskin and Daniel V. Schroeder. *An Introduction to quantum field theory.* Addison-Wesley, Reading, USA, 1995.

[34] H.David Politzer. Asymptotic Freedom: An Approach to Strong Interactions. *Phys. Rept.*, 14:129–180, 1974.

[35] L.E. Price, J.R. Dunning, M. Goitein, K. Hanson, T. Kirk, and R. Wilson. Backward-angle electron-proton elastic scattering and proton electromagnetic form-factors. *Phys. Rev. D*, 4:45–53, 1971.

[36] I. A. Qattan, J. Arrington, R. E. Segel, X. Zheng, K. Aniol, O. K. Baker, R. Beams, E. J. Brash, J. Calarco, A. Camsonne, J.-P. Chen, M. E. Christy, D. Dutta, R. Ent, S. Frullani, D. Gaskell, O. Gayou, R. Gilman, C. Glashausser, K. Hafidi, J.-O. Hansen, D. W. Higinbotham, W. Hinton, R. J. Holt, G. M. Huber, H. Ibrahim, L. Jisonna, M. K. Jones, C. E. Keppel, E. Kinney, G. J. Kumbartzki, A. Lung, D. J. Margaziotis, K. McCormick, D. Meekins, R. Michaels, P. Monaghan, P. Moussiegt, L. Pentchev, C. Perdrisat, V. Punjabi, R. Ransome, J. Reinhold, B. Reitz, A. Saha, A. Sarty, E. C. Schulte, K. Slifer, P. Solvignon, V. Sulkosky, K. Wijesooriya, and B. Zeidman. Precision rosenbluth measurement of the proton elastic form factors. *Phys. Rev. Lett.*, 94:142301, Apr 2005.

[37] Wallon Samuel. Hard exclusive processes in pertubative qcd: from medium to asymptotical energies, June 2017. Laboratoire de Physique Théorique, Université Paris-Sud and Université Pierre et Marie Curie.

[38] M.D. Schwartz. *Quantum Field Theory and the Standard Model.* Quantum Field Theory and the Standard Model. Cambridge University Press, 2014.

[39] A. F. Sill, R. G. Arnold, P. E. Bosted, C. C. Chang, J. Gomez, A. T. Katramatou, C. J. Martoff, G. G. Petratos, A. A. Rahbar, S. E. Rock, Z. M. Szalata, D. J. Sherden, J. M. Lambert, and R. M. Lombard-Nelsen. Measurements of elastic electron-proton scattering at large momentum transfer. *Phys. Rev. D*, 48:29–55, Jul 1993.

[40] G.G. Simon, Ch. Schmitt, F. Borkowski, and V.H. Walther. Absolute electron-proton cross sections at low momentum transfer measured with a high pressure gas target system. *Nuclear Physics A*, 333(3):381 – 391, 1980.

[41] George F. Sterman and Steven Weinberg. Jets from Quantum Chromodynamics. *Phys. Rev. Lett.*, 39:1436, 1977.

[42] A. Ghaffari Tooran, A. Khorramian, and H. Abdolmaleki. Qcd analysis of structure functions in deep inelastic neutrino-nucleon scattering without using the orthogonal polynomials approach. *Physical Review C*, 99(3), 2019.

[43] R. C. Walker, B. W. Filippone, J. Jourdan, R. Milner, R. McKeown, D. Potterveld, L. Andivahis, R. Arnold, D. Benton, P. Bosted, G. deChambrier, A. Lung, S. E. Rock, Z. M. Szalata, A. Para, F. Dietrich, K. Van Bibber, J. Button-Shafer, B. Debebe, R. S. Hicks, S. Dasu, P. de Barbaro, A. Bodek, H. Harada, M. W. Krasny, K. Lang, E. M. Riordan, R. Gearhart, L. W. Whitlow, and J. Alster. Measurements of the proton elastic form factors for $1 \leq Q^2 \leq 3$ $(\mathrm{GeV}/c)^2$ at slac. *Phys. Rev. D*, 49:5671–5689, Jun 1994.